

Differentiable Singular Value Decomposition (SVD)

Rohit Sunil Kanchi^a, Sicheng He^a

^a*Department of Mechanical, Aerospace, and Biomedical Engineering, University of Tennessee, Knoxville, TN 37996, USA*

Abstract

Singular value decomposition (SVD) is widely used in modal analysis, such as proper orthogonal decomposition (POD) and resolvent analysis, to extract key features from complex problems. SVD derivatives need to be computed efficiently to enable the large-scale design optimization. However, for a general complex matrix, no method can accurately compute this derivative to machine precision and remain scalable with respect to the number of design variables without requiring the all of the singular variables. We propose two algorithms to efficiently compute this derivative based on the adjoint method and reverse automatic differentiation (RAD) and RAD-based singular value derivative formula. Differentiation results for each method proposed were compared with FD results for one square and one tall rectangular matrix example and matched with the FD results to about 5–7 digits. Finally, we demonstrate the scalability of the proposed method by calculating the derivatives of singular values with respect to the snapshot matrix derived from the POD of a large dataset for a laminar-turbulent transitional flow over a flat plate, sourced from the John Hopkins turbulence database (JHTDB).

1. Introduction

Singular variable decomposition (SVD) is a fundamental linear algebra technique widely used in engineering applications [1, 2]. SVD is applied in varied fields such as numerical optimization [3], mechanical design [4, 5, 6, 7, 8], fluid dynamics [9, 10], noise-reduction [11, 12, 13], image processing [14], and finance [15]. Applications of SVD in engineering optimization and analysis problems include aerostructural optimization [16, 17, 18], aerodynamic shape optimization [19, 20, 21, 22, 23, 24] and pure structural optimization problems [25, 26, 27, 28]. Many modal analysis methods are based

on SVD, e.g., the resolvent analysis [29], and dynamic mode decomposition (DMD) [30]. For more details about SVD in modal analysis, see the review papers by Taira et al. [31, 32].

There are several routes to compute SVD of a given matrix (refer to Golub and Van Loan [33, Chapter 8.6] for more details). A popular approach is to reduce the problem to an eigenvalue problem (EVP) [33, 34]. Once that is done, numerical methods such as Golub-Kahan bi-diagonalization [33] and the Jacobi SVD algorithm [35] can be used to compute the SVD. Iterative but approximating methods such as Lanczos or Krylov subspace methods [36], randomized SVD [37], and truncated SVD have also been developed to reduce computational costs, particularly for large-scale data or high-dimensional systems.

These advancements are crucial when differentiation of the SVD is needed, as the computational cost and numerical stability of differentiation depend heavily on the underlying method used to compute the SVD. This motivates the need to carefully evaluate SVD computation strategies for their efficiency and compatibility with different differentiation frameworks. For a more thorough review of SVD history and algorithms, especially the relationship between EVP and SVD, we direct readers to the review by Zhang [38] and Lecture 31 of Trefethen and Bau [34].

Two approaches in the relationship between the EVP of a symmetric matrix and the SVD were leveraged in the current study. In the first approach, we perform eigendecomposition of the product of the matrix and its Hermitian transpose (if real, just transpose), and the reverse product [33, 34, 39]. The resulting matrices from this pair of products are the Gram matrices [40, 34, 41] of the matrix under consideration whose SVD is sought, or in other words, the target matrix. The eigendecomposition of the Gram matrix resulting from the product of the target matrix and its Hermitian transpose gives the singular values and the left singular vectors of the SVD. Here, the eigenvectors are the left singular vectors, and the square roots of the eigenvalues are the singular values. Similarly, the eigendecomposition of the Gram matrix from the product of the reverse product of the target matrix and its Hermitian transpose yields the singular values and the right singular vectors of the target matrix [33]. We developed governing equations for this approach based on the approach taken by He et al. [42]. This approach is useful when the matrix whose SVD is sought is sparse. If it is dense, then forming the left or right Gram matrices is costly, which motivated the second approach.

In the second approach, we leverage the relationship between the SVD

of the target matrix and the EVP of its symmetric embedding [33, 43]. The relationship is such that the singular value and its negative counterpart are eigenvalues of the symmetric embedding. The eigenvectors of the symmetric embedding contain the left and right singular vectors of the target matrix. We developed a set of SVD governing equations in the current manuscript based on this symmetric embedding which can be solved using an alternating least squares approach with Rayleigh quotient through successive deflation [33, 34, 44].

The derivative computation methods proposed in the current manuscript are not limited to only the EVP-SVD approach to compute the singular variables. So long as the singular variables computed through any algorithm satisfy the governing equations for either aforementioned case, the proposed derivative algorithms will work. However, there arise problems whose solutions might involve nearly similar or duplicated singular values [33, 45, 46]. Since the singular values are the square roots of the eigenvalues of the Gram matrices, the Gram matrices EVPs yield repeated eigenvalues in the case of duplicate singular values. Typically, such duplicated or close eigenvalues occur due to some spatial symmetry in the problem whose eigen-solution is sought [47, 48]. It is a fact that the changes of the order of ϵ in a matrix can alter its singular subspace by δ/ϵ where δ is a measure of how far apart the singular values are from each other (refer to Golub and Van Loan [33, Chapter 8.6.1]). Thus, if two singular values are close or the same, the ratio would tend to infinitely large values. This means that the singular vector space is mathematically degenerate [48]. Angelova and Petkov [46] showed in a component-wise perturbation analysis that the SVD perturbation problem is only well-posed when the singular values are distinct. The distinct singular values, therefore, ensure uniqueness in solution to the governing equations developed. This case of duplicate singular values is, however, beyond the scope of the current manuscript.

Once the required singular variables are obtained from either of the two EVP-SVD approaches mentioned, the derivative of the singular variables is sought, which has applications in different design optimization problems. For instance, Ersoy and Mugan [27] computed the derivatives of the singular values and vectors for the structural design derivative analysis. Santiago et al. [49] took the derivatives of the singular values of the shapes in the shape derivative as part of the shape optimization for photonic nanostructures. Recently, Skene and Schmid [50] performed a mixed forward and backward derivative analysis for the swirling M-flames, which involved computation of

the resolvent with respect to the design parameters. The resolvent analysis involved the singular value decomposition of the resolvent matrix, which gave the dominant singular value whose derivative was sought.

Various methods are used for computing derivatives, including finite differences (FD), complex step (CS), algorithmic differentiation (AD), the direct method, and the adjoint method (refer to Martins and Ning [51, Chapter 6]). These methods differ in terms of their accuracy and computational efficiency. Efficiency-wise, each method is typically optimized for either scaling with the number of outputs (e.g., functions of interest such as eigenvalues and eigenvectors) or the number of inputs (e.g., design variables), but rarely both [52],[51, Chapter 6].

FD is susceptible to truncation and subtraction errors, whereas CS avoids these issues with a sufficiently small step size and can achieve machine precision [53]. FD and CS are relatively easy to implement due to their black-box-like nature. However, these methods may not be practical for high-fidelity applications involving a large number of design variables. (For a detailed comparison of FD and the adjoint method, refer to [54] and [51, Chapter 6] (Fig. 6.43)). Further, their computational cost scales unfavourably with the number of inputs, with CS being more expensive because of the use of complex arithmetic. For instance, with respect to differentiating SVD, Ersoy, and Mugan [27] computed the SVD derivatives using the FD approach, which lacks both accuracy and scalability with respect to design variables. This motivates us to choose a method that does not scale with a number of inputs.

AD differentiates a program based on the systematic application of the chain rule. Forward-AD (FAD) does this by applying the chain rule from inputs to the outputs, and reverse-AD (RAD) does so in the reverse order. Thus, the cost is proportional to the number of inputs when FAD is implemented and the number of outputs when RAD is used. Currently, for derivative algorithms that do not scale with inputs, there are only RAD-based methods in the literature to compute the SVD derivative [55, 56, 57, 58]. The RAD formula proposed by Giles [55] works for only real values. The RAD form proposed by Townsend [56] works for real values and works with reduced SVD. Santiago et al. [49] took the derivatives of the singular values for the shape optimization for photonic nanostructures by using the RAD formula given for real-valued SVD by Townsend [56]. Wan and Zhang [58] proposed a RAD formula for the full SVD that works with complex-valued inputs. Finally, Seeger et al. [57] proposed a formula equiv-

alent to Townsend’s [56]. However, these methods require all of the singular variables during the derivative computation. This increases the computational storage required, which motivates the proposal of a method that does not involve several large matrix-matrix products and computes the derivative more memory-efficiently. Projection-based method was developed by He et al. [59] to partially address this challenge in eigenvector derivative computation.

Beyond explicit analytic methods like AD, implicit analytic methods like direct and adjoint approaches can also be used [51, Chapter 6]. The efficiency of these methods depends on the relative number of inputs and outputs. The direct method is preferable when the number of inputs is smaller than the number of outputs. In contrast, the adjoint method is more efficient when the number of inputs exceeds the number of outputs. Skene and Schmid [50], for instance, used the direct approach to compute the resolvent derivative. However, this scales inefficiently with the number of inputs. Further, there are no adjoint-based methods to compute the SVD derivative.

To address the aforementioned challenges, we develop an adjoint and RAD-based method to compute the derivative efficiently. The contribution of the current manuscript is summarized as follows: (1) We develop two adjoint-based approaches to compute the derivative of the SVD problem for general complex (square and rectangular) matrices. In the first approach, we leverage the relationship between the EVP of the Gram matrices of the SVD of the target matrix. In the second approach, we leverage the relationship between the EVP of the target matrix’s symmetric embedding and the target matrix’s SVD. The proposed adjoint techniques can calculate the derivative to machine precision, are straightforward to implement, do not scale with the number of design variables (inputs), and are suitable for use in gradient-based optimization involving SVD. (2) We develop a RAD-based analytic formula to compute the singular value derivative with respect to a complex input matrix, which also works with real-valued matrices in a reduced form. (3) We propose a generic dot product identity as a tool to derive complex-valued RAD derivative formulae using FAD derivative formulae for complex differentiable functions.

The manuscript is organized as follows. In Section 2, we present the governing equations for the two proposed adjoint method-based approaches for computing the SVD derivative. Here, the first method relies on forming one of the two Gram-matrices of the main matrix whose SVD derivative is sought. The second method is based on the symmetric embedding of the tar-

get matrix, as mentioned. In Section 3, we propose these two adjoint-based approaches and a general RAD-based formula for singular value derivative. In Section 4, we compare the results from our proposed adjoint methods and RAD formula for singular value derivative with FD for two randomly selected complex matrices, one square and one rectangular. Next, we show the scalability by testing the singular value derivative on a large dataset sourced from the John Hopkins turbulence database (JHTDB) [60], which was the transition to turbulence dataset of flow over a flat plate. Finally, we present our conclusions in Section 5. We present a summary of the contributions of researchers in differentiating the SVD and our contributions in Table 1.

2. Governing equations

SVD for a general complex matrix $\mathbf{A} \in \mathbb{C}^{m \times n}$ is defined as

$$\mathbf{A} = \mathbf{U}\mathbf{\Sigma}\mathbf{V}^*, \quad (1)$$

where $\mathbf{U} \in \mathbb{C}^{m \times m}$ is the matrix of left singular vectors with each column being a left singular vector, $\mathbf{V} \in \mathbb{C}^{n \times n}$ is the matrix of right singular vectors with each column being a left singular vector, $\mathbf{\Sigma} \in \mathbb{R}^{m \times n}$ is a rectangular matrix of singular values on the main diagonal and zeros elsewhere represented by σ_i on the main diagonal, arranged in descending order, i.e., $\sigma_1 \geq \sigma_2 \geq \dots \geq \sigma_n \geq 0$, \square^* denotes the Hermitian transpose of a complex matrix, $m, n \in \mathbb{Z}^+$ are the problem size (without loss of generality, we assume $m > n$).

The SVD and EVP are closely related problems. There are two ways to compute the singular value via solving an EVP. The first approach uses the two Gram matrices $\mathbf{B} = \mathbf{A}\mathbf{A}^* \in \mathbb{C}^{m \times m}$ and $\mathbf{C} = \mathbf{A}^*\mathbf{A} \in \mathbb{C}^{n \times n}$ (refer to Schwerdtfeger [40, Page 141] and to Makkonen and Hollanti [41]). Thus, we name it *Gram matrix method* (GMM). The second approach is *Symmetric embedding matrix method* (SEMM) (refer to Golub and Van Loan [33, Chapter 8.6] and Ragnarsson and Van Loan [43]). We elaborate on these two approaches in the following Sections 2.1 and 2.2.

2.1. Gram matrix method (GMM)

It can be shown that the singular vectors and singular values can be obtained from \mathbf{B} and \mathbf{C} (See Golub and Van Loan [33, Chapter 8.6])

$$\begin{aligned} \mathbf{B} &= \mathbf{A}\mathbf{A}^* = \mathbf{U}\mathbf{\Sigma}\mathbf{V}^*\mathbf{V}\mathbf{\Sigma}\mathbf{U}^* = \mathbf{U}\mathbf{\Sigma}^2\mathbf{U}^*, \\ \mathbf{C} &= \mathbf{A}^*\mathbf{A} = \mathbf{V}\mathbf{\Sigma}\mathbf{U}^*\mathbf{U}\mathbf{\Sigma}\mathbf{V}^* = \mathbf{V}\mathbf{\Sigma}^2\mathbf{V}^*. \end{aligned} \quad (2)$$

Table 1: Summary of contributions in literature and current manuscript for SVD derivative computation

Equations	Uses only required singular variables ^a	Singular value derivative	Singular vector derivative	Works for complex-valued inputs	Author (s)
$\bar{\mathbf{A}} = \mathbf{U}\bar{\mathbf{S}}\mathbf{V}^\top$	✗	✓	✗	✗	Eq. (K.1) Giles [61]
$\bar{\mathbf{A}} = [\mathbf{U}(\mathbf{F} \circ [\mathbf{U}^\top \bar{\mathbf{U}} - \bar{\mathbf{U}}^\top \mathbf{U}])\mathbf{S}$ $+ (\mathbf{I}_m - \mathbf{U}\mathbf{U}^\top)\bar{\mathbf{U}}\mathbf{S}^{-1}]\mathbf{V}^\top$ $+ \mathbf{U}(\mathbf{I}_k \circ \bar{\mathbf{S}})\mathbf{V}^\top$ $\mathbf{U}[\mathbf{S}(\mathbf{F} \circ [\mathbf{V}^\top \bar{\mathbf{V}} - \bar{\mathbf{V}}^\top \mathbf{V}])\mathbf{V}^\top$ $+ \mathbf{S}^{-1}\bar{\mathbf{V}}^\top(\mathbf{I}_n - \mathbf{V}\mathbf{V}^\top)]$	✗	✓	✓	✗	Eq. (K.2) Townsend [56]
$\bar{\mathbf{A}} = \frac{1}{2}(2\mathbf{U}\bar{\mathbf{S}}\mathbf{V}^* + \mathbf{U}(\mathbf{J} + \mathbf{J}^*)\mathbf{S}\mathbf{V}^*$ $+ \mathbf{U}\mathbf{S}(\mathbf{K} + \mathbf{K}^*)\mathbf{V}^* + \frac{1}{2}\mathbf{U}\mathbf{S}^{-1}(\mathbf{L}^* - \mathbf{L})\mathbf{V}^*$ $+ 2(\mathbf{I} - \mathbf{U}\mathbf{U}^*)\bar{\mathbf{U}}\mathbf{S}^{-1}\mathbf{V}^*$ $+ 2\mathbf{U}\mathbf{S}^{-1}\bar{\mathbf{V}}^*(\mathbf{I} - \mathbf{V}\mathbf{V}^*))$	✗	✓	✓	✓	Eq. (K.4) Wan and Zhang [58]
$\bar{\mathbf{A}} = \mathbf{U}^\top(\mathbf{G}_2\mathbf{V} + \Lambda^{-1}\bar{\mathbf{V}})$, $\mathbf{G}_2 = \bar{\Lambda} + 2\mathit{sym}(\mathbf{G}_1 \circ \mathbf{E})\Lambda$ $- (\Lambda^{-1}\bar{\mathbf{V}}\mathbf{V}^\top \circ \mathbf{I})$, $\mathbf{G}_1 = \bar{\mathbf{U}}\mathbf{U}^\top + \Lambda^{-1}\bar{\mathbf{V}}\mathbf{V}^\top\Lambda$	✗	✗	✓	✗	Eq. (K.5) Seeger et al. [57]
$\mathbf{M}_g^\top \psi_g = (\partial g / \partial \mathbf{w})^\top$ $\mathbf{M}_h^\top \psi_h = (\partial h / \partial \mathbf{w})^\top$	✓	✓	✓	✓	Eqs. (16) and (21)
$\mathbf{M}_f^\top \psi_f = (\partial f / \partial \mathbf{w})^\top$	✓	✓	✓	✓	Eq. (26)
$\bar{\mathbf{A}}_r = (\mathbf{u}_r \mathbf{v}_r^\top + \mathbf{u}_i \mathbf{v}_i^\top) \bar{\sigma}$ $\bar{\mathbf{A}}_i = (-\mathbf{u}_r \mathbf{v}_i^\top + \mathbf{u}_i \mathbf{v}_r^\top) \bar{\sigma}$	✓	✓	✗	✓	Eq. (30)

^aRequires only σ , \mathbf{u} and/or \mathbf{v} for the derivative calculations, not all the singular variables inside matrices \mathbf{U} , Σ and/or \mathbf{V}

Thus, the left singular vectors, \mathbf{U} , are just the eigenvectors obtained from the eigen-decomposition of \mathbf{B} and the right singular vectors, \mathbf{V} , are the eigenvectors obtained from the eigen-decomposition of \mathbf{C} . The first few singular values are taken from the common eigenvalues between \mathbf{B} and \mathbf{C} . The remaining singular values are taken from the remaining eigenvalues depending on whether \mathbf{A} is tall or wide.

To apply adjoint method to compute the derivative, we need to construct the residual form of the EVP. Consider an EVP of a general complex square matrix, $\mathbf{D} \in \mathbb{C}^{m \times m}$, we have

$$\mathbf{D}\phi = \lambda\phi, \quad (3)$$

where λ and ϕ is one eigen-pair. In general, the eigenvalues and vectors are complex. It is assumed that the eigenvalues are distinct and hence have multiplicity of one. To obtain unique complex eigenvectors, we consider the following set of governing equations, in conjunction with Eq. (3). The residual form is (see He et al. [42] for more detail)

$$\mathbf{r}(\mathbf{w}) = \begin{bmatrix} \mathbf{D}\phi - \lambda\phi \\ \phi^*\phi - 1 \\ \text{Im}(\phi_k) \end{bmatrix}, \quad \mathbf{w} = \begin{bmatrix} \lambda \\ \phi \end{bmatrix}, \quad (4)$$

where we further require that $\text{Re}(\phi_k) > 0$, $k = \text{argmax}_j \|\phi_j\|_2$, and ϕ_k is the k^{th} element of the vector ϕ . This is required because the complex eigenvector can always be scaled and rotated in the complex plane. If we apply stretching and rotation in this plane, we obtain:

$$\mathbf{D}(\alpha\phi e^{i\theta}) = \lambda(\alpha\phi e^{i\theta}), \quad (5)$$

where $\alpha \in \mathbb{R}$ (scaling factor), $\theta \in \mathbb{R}$ (rotation angle).

The last two equations from Eq. (4) therefore constrain the norm of the eigenvector to be one, and constrains the angle of the eigenvector.

Rewriting the Eq. (4) by splitting into their respective real and imaginary parts, we have

$$\mathbf{r}(\mathbf{w}) = \begin{bmatrix} r_{\text{main,r}} \\ r_{\text{main,i}} \\ r_m \\ r_p \end{bmatrix} = \begin{bmatrix} \mathbf{D}_r\phi_r - \mathbf{D}_i\phi_i - \lambda_r\phi_r + \lambda_i\phi_i \\ \mathbf{D}_i\phi_r + \mathbf{D}_r\phi_i - \lambda_i\phi_r - \lambda_r\phi_i \\ \phi_r^T\phi_r + \phi_i^T\phi_i - 1 \\ e_k^T\phi_i \end{bmatrix}, \quad \mathbf{w} = \begin{bmatrix} \phi_r \\ \phi_i \\ \lambda_r \\ \lambda_i \end{bmatrix}, \quad (6)$$

where \mathbf{e}_k is a vector with all zero elements except that k^{th} element equal to one.

For SVD, we can leverage Eq. (2) to convert it to an EVP. In Eq. (6), we can set $\mathbf{D} = \mathbf{B}$, then we have a governing equation for the left singular vector and singular value. In this case, the left singular value becomes the square root of λ and the corresponding left singular vector is simply equal to ϕ in Eq. (3). We call this the *Left Gram Matrix Method* (LGMM) since it is the Gram matrix associated with the left singular values.

Alternatively, if we set $\mathbf{D} = \mathbf{C}$, we have a governing equation for the right singular vector and singular value. Again, in this case, the right singular value becomes the square root of λ and the corresponding right singular vector is simply equal to ϕ in Eq. (3). We call this the *Right Gram Matrix Method* (RGMM) since it is the Gram matrix associated with the right singular values.

2.2. Symmetric embedding matrix method

This second approach leverages the following relationship

$$\begin{bmatrix} \mathbf{O} & \mathbf{A} \\ \mathbf{A}^* & \mathbf{O} \end{bmatrix} \begin{bmatrix} \mathbf{u}_i \\ \mathbf{v}_i \end{bmatrix} = \pm \sigma_i \begin{bmatrix} \mathbf{u}_i \\ \mathbf{v}_i \end{bmatrix}, \quad (7)$$

where σ_i , \mathbf{u}_i and \mathbf{v}_i is one group of singular value and singular vectors (refer to Golub and Van Loan [33, Chapter 8.6] and Ragnarsson and Van Loan [43]). Thus, by applying these identities Eqs. (2) and (7), we can obtain the nonlinear governing equations for SVD with additional normalization condition constraints.

In the previous Section 2.1, we develop a formulation that relies on the evaluation of \mathbf{B} or \mathbf{C} to convert the problem to an EVP where the left or right singular vectors for the corresponding singular value are computed. The main drawback of that method is that the evaluation of matrix product, $\mathbf{B} = \mathbf{A}\mathbf{A}^*$ or $\mathbf{C} = \mathbf{A}^*\mathbf{A}$, can be expensive when the coefficient matrix is dense. This motivates us to develop an alternative formulation that is matrix-product free.

We developed the following equation. By solving this equation, we can get the left, and right singular vectors, and singular value in one shot. The

equation is

$$\begin{aligned}
\mathbf{A}\mathbf{v} &= \sigma\mathbf{u}, \\
\mathbf{A}^*\mathbf{u} &= \sigma\mathbf{v}, \\
\mathbf{u}^*\mathbf{u} &= 1, \\
\text{Im}(\mathbf{u}_k) &= 0.
\end{aligned} \tag{8}$$

Notice that by constraining the left singular vector \mathbf{u} , we end up constraining the right singular vector \mathbf{v} .

Starting from Eq. (8), we can split it into real and imaginary parts and write the residual form as

$$\mathbf{r}(\mathbf{w}) = \begin{bmatrix} \mathbf{A}_r\mathbf{v}_r - \mathbf{A}_i\mathbf{v}_i - \sigma_r\mathbf{u}_r + \sigma_i\mathbf{u}_i \\ \mathbf{A}_r\mathbf{v}_i + \mathbf{A}_i\mathbf{v}_r - \sigma_r\mathbf{u}_i - \sigma_i\mathbf{u}_r \\ \mathbf{A}_r^\top\mathbf{u}_r + \mathbf{A}_i^\top\mathbf{u}_i - \sigma_r\mathbf{v}_r + \sigma_i\mathbf{v}_i \\ \mathbf{A}_r^\top\mathbf{u}_i - \mathbf{A}_i^\top\mathbf{u}_r - \sigma_r\mathbf{v}_i - \sigma_i\mathbf{v}_r \\ \mathbf{u}_r^\top\mathbf{u}_r + \mathbf{u}_i^\top\mathbf{u}_i - 1 \\ \mathbf{e}_k^\top\mathbf{u}_i \end{bmatrix}, \quad \mathbf{w} = \begin{bmatrix} \mathbf{u}_r \\ \mathbf{u}_i \\ \mathbf{v}_r \\ \mathbf{v}_i \\ \sigma_r \\ \sigma_i \end{bmatrix}, \tag{9}$$

where \mathbf{w} is the state vector. It is well-known that the singular value, σ , is real. However, here we relax it to be a complex number to have equal numbers of equations and unknowns.

Now, we prove that the solution of Eq. (8) is indeed a SVD pair. Pre-multiplying the first equation of Eq. (8) by \mathbf{u}^* , we have

$$\mathbf{u}^*\mathbf{A}\mathbf{v} = \sigma\mathbf{u}^*\mathbf{u} = \sigma. \tag{10}$$

Then, we pre-multiply the second equation of Eq. (8) by \mathbf{v}^* , we have

$$\mathbf{v}^*\mathbf{A}^*\mathbf{u} = \sigma\mathbf{v}^*\mathbf{v} = \sigma\|\mathbf{v}\|_2. \tag{11}$$

Then, realizing that the Eqs. (10) and (11) are conjugate transpose, we have

$$\sigma^* = \sigma\|\mathbf{v}\|_2 \Rightarrow \sigma_r = \|\mathbf{v}\|_2\sigma_r, -\sigma_i = \|\mathbf{v}\|_2\sigma_i, \tag{12}$$

we have as long as $\sigma = 0$, or $\|\mathbf{v}\|_2 = 1$ and $\sigma_i = 0$. Thus, we have implicitly enforced that σ is real.

2.3. Discussion

The difference between the two formulations GMM and SEMM is that using Eq. (2) method, we can formulate a smaller dimension problem (e.g. if

we have $m > n$, we can form \mathbf{C} which is $n \times n$). However, the disadvantage of this method is that it only computes one singular vector (left or right) and singular value, and the other singular vector (right or left) needs to be recovered. Another disadvantage is that Eq. (2) requires computing matrix-product. If the matrix is dense, it can be prohibitively expensive to compute this product.

On the other hand, the conversion using Eq. (7) has the advantage that it does not require the matrix product needed in the previous matrix-product formulation. In addition, the equation includes the singular value and the corresponding left and right singular vectors. Thus, we do not need to conduct additional computation to search the other singular vector as required by Eq. (2) method. The disadvantage of this method is that the problem size ($m+n$) is larger than the Eq. (2) method. We also ensure that there are no repeated singular values else the singular vector space becomes degenerate [33, 48].

3. Derivative computation

In this section, we propose two general methods to compute the derivative of any function of the singular variables with respect to a general complex matrix, \mathbf{A} . We also propose an RAD formula for just the singular value derivative. The section is organized as follows: In Section 3.1, a brief introduction to the adjoint method is given. Section 3.2 then gives the adjoint method applied to the governing equations resulting from GMM. Similarly in Section 3.3, the adjoint method is applied to the governing equations resulting from the SEMM. Finally, in Section 3.4, we propose the RAD formula for the singular value derivative for both complex and real-valued cases.

3.1. Adjoint method

For arbitrary function of interest, $f(\mathbf{w}, \mathbf{x})$, we can use the adjoint method to compute its total derivative with respect to \mathbf{x} . The total derivative is computed using the following formula [51]

$$\frac{df}{d\mathbf{x}} = \frac{\partial f}{\partial \mathbf{x}} - \boldsymbol{\psi}^\top \frac{\partial \mathbf{r}}{\partial \mathbf{x}}. \quad (13)$$

The adjoint vector, $\boldsymbol{\psi}$, can be found by solving the system of equations resulting from the following adjoint equation

$$\frac{\partial \mathbf{r}^\top}{\partial \mathbf{w}} \boldsymbol{\psi} = \frac{\partial f^\top}{\partial \mathbf{w}}, \quad (14)$$

where $\mathbf{r} = \mathbf{r}(\mathbf{w})$ is the residual vector for the governing equation (Eq. (4)), \mathbf{w} being the state variables vector. We direct the readers to He et al. [42] for the complete adjoint method to solving the EVP derivative. For the summary of the equations and algorithm, see Appendix A.

For the SVD problem, our objective function now becomes:

$$f = f(\mathbf{u}, \mathbf{v}, \sigma, \mathbf{A}), \quad (15)$$

where f can be any function of the singular variables: \mathbf{u} which is the left singular vector, \mathbf{v} the right singular vector and these vectors correspond to a chosen singular value (typically the dominant one) σ . \mathbf{A} is also placed in the objective function for the general case if there are any direct dependencies on it, as will be seen in forthcoming sections.

3.2. Adjoint equation of GMM

The computation of the derivative of a general function, $f(\mathbf{u}, \mathbf{v}, \sigma, \mathbf{A})$, can be decomposed into two steps. Before we begin with the computation of the derivative of $f(\mathbf{u}, \mathbf{v}, \sigma, \mathbf{A})$ with respect to \mathbf{A} , consider first the derivatives of $g(\mathbf{u}, \sigma, \mathbf{A})$ and $h(\mathbf{v}, \sigma, \mathbf{A})$. If the function is $g(\mathbf{u}, \sigma, \mathbf{A})$, it is related to the matrix \mathbf{B} . If the function is $h(\mathbf{v}, \sigma, \mathbf{A})$, it is related to the matrix $\mathbf{C} = \mathbf{A}^* \mathbf{A}$ (Refer Section 2.1). We split this function f into its real and imaginary components as g_r and g_i for the function g and h_r and h_i for the function h and therefore we must solve the adjoint for a total of two times for each of g and h , once for real part and once for imaginary part of each of g and h . This is done to save computational effort as will be seen in the forthcoming section. We present this approach as follows.

3.2.1. Adjoint equation of LGMM

We found the adjoint equation for the function $g = g(\mathbf{u}, \sigma, \mathbf{A}) \in \mathbb{R}$ to be

$$\mathbf{M}_g^\top \boldsymbol{\psi}_g = \frac{\partial g^\top}{\partial \mathbf{w}}, \quad (16)$$

where \mathbf{M}_g is

$$\mathbf{M}_g = \begin{bmatrix} \mathbf{B}_r - \lambda_r \mathbf{I} & -\mathbf{B}_i + \lambda_i \mathbf{I} & -\mathbf{u}_r & \mathbf{u}_i \\ \mathbf{B}_i - \lambda_i \mathbf{I} & \mathbf{B}_r + \lambda_r \mathbf{I} & -\mathbf{u}_i & -\mathbf{u}_r \\ 2\mathbf{u}_r^\top & 2\mathbf{u}_i^\top & 0 & 0 \\ 0 & \mathbf{e}_k^\top & 0 & 0 \end{bmatrix}, \quad (17)$$

and $\boldsymbol{\psi}_g$ is

$$\boldsymbol{\psi}_g = \begin{bmatrix} \boldsymbol{\psi}_{g,r} \\ \boldsymbol{\psi}_{g,i} \\ \boldsymbol{\psi}_{m,g} \\ \boldsymbol{\psi}_{p,g} \end{bmatrix}, \quad (18)$$

and once the solution to the adjoint vector $\boldsymbol{\psi}$ from either approach is obtained, we can proceed to compute the total derivatives using Eq. (13).

We assumed that function g outputs a real number, i.e., $g \in \mathbb{R}$. If otherwise, function g returns a complex number, i.e., $g \in \mathbb{C}$, we can break it into its real and imaginary parts and apply Eq. (16) twice. We now have two adjoint vectors, namely: $\boldsymbol{\psi}_{g_r}$ and $\boldsymbol{\psi}_{g_i}$ for the function g , each with its real and imaginary parts. The derivative of the residual vector \mathbf{r} for the function g with respect to the matrix \mathbf{B} is then

$$\begin{aligned} \frac{\partial \mathbf{r}_{g_r}^\top}{\partial \mathbf{B}_r} \boldsymbol{\psi}_{g_r} &= \boldsymbol{\psi}_{g_r,r} \mathbf{u}_r^\top + \boldsymbol{\psi}_{g_r,i} \mathbf{u}_i^\top, \\ \frac{\partial \mathbf{r}_{g_r}^\top}{\partial \mathbf{B}_i} \boldsymbol{\psi}_{g_r} &= -\boldsymbol{\psi}_{g_r,r} \mathbf{u}_i^\top + \boldsymbol{\psi}_{g_r,i} \mathbf{u}_r^\top, \\ \frac{\partial \mathbf{r}_{g_i}^\top}{\partial \mathbf{B}_r} \boldsymbol{\psi}_{g_i} &= \boldsymbol{\psi}_{g_i,r} \mathbf{u}_r^\top + \boldsymbol{\psi}_{g_i,i} \mathbf{u}_i^\top, \\ \frac{\partial \mathbf{r}_{g_i}^\top}{\partial \mathbf{B}_i} \boldsymbol{\psi}_{g_i} &= -\boldsymbol{\psi}_{g_i,r} \mathbf{u}_i^\top + \boldsymbol{\psi}_{g_i,i} \mathbf{u}_r^\top, \end{aligned} \quad (19)$$

A detailed derivation for this formula can be found in the paper by He et al. [42]. To proceed to the derivative with respect to the matrix \mathbf{A} , we apply chain rule via the reverse automatic differentiation formula (See Appendix B for derivation). Thus, to compute the derivatives of the function $f = g$

with respect to matrix \mathbf{A} , we have

$$\begin{aligned}
\frac{df_r}{d\mathbf{A}_r} &= -\left(\frac{\partial \mathbf{r}_{g_r}^\top}{\partial \mathbf{B}_r} \boldsymbol{\psi}_{g_r}\right) \mathbf{A}_r - \left(\frac{\partial \mathbf{r}_{g_r}^\top}{\partial \mathbf{B}_r} \boldsymbol{\psi}_{g_r}\right)^\top \mathbf{A}_r - \left(\frac{\partial \mathbf{r}_{g_r}^\top}{\partial \mathbf{B}_i} \boldsymbol{\psi}_{g_r}\right)^\top \mathbf{A}_i \\
&\quad + \left(\frac{\partial \mathbf{r}_{g_r}^\top}{\partial \mathbf{B}_i} \boldsymbol{\psi}_{g_r}\right) \mathbf{A}_i + \frac{\partial f_r}{\partial \mathbf{A}_r}, \\
\frac{df_i}{d\mathbf{A}_r} &= -\left(\frac{\partial \mathbf{r}_{g_i}^\top}{\partial \mathbf{B}_r} \boldsymbol{\psi}_{g_i}\right) \mathbf{A}_r - \left(\frac{\partial \mathbf{r}_{g_i}^\top}{\partial \mathbf{B}_r} \boldsymbol{\psi}_{g_i}\right)^\top \mathbf{A}_r - \left(\frac{\partial \mathbf{r}_{g_i}^\top}{\partial \mathbf{B}_i} \boldsymbol{\psi}_{g_i}\right)^\top \mathbf{A}_i \\
&\quad + \left(\frac{\partial \mathbf{r}_{g_i}^\top}{\partial \mathbf{B}_i} \boldsymbol{\psi}_{g_i}\right) \mathbf{A}_i + \frac{\partial f_i}{\partial \mathbf{A}_r}, \\
\frac{df_r}{d\mathbf{A}_i} &= -\left(\frac{\partial \mathbf{r}_{g_r}^\top}{\partial \mathbf{B}_r} \boldsymbol{\psi}_{g_r}\right) \mathbf{A}_i - \left(\frac{\partial \mathbf{r}_{g_r}^\top}{\partial \mathbf{B}_r} \boldsymbol{\psi}_{g_r}\right)^\top \mathbf{A}_i - \left(\frac{\partial \mathbf{r}_{g_r}^\top}{\partial \mathbf{B}_i} \boldsymbol{\psi}_{g_r}\right)^\top \mathbf{A}_r \\
&\quad + \left(\frac{\partial \mathbf{r}_{g_r}^\top}{\partial \mathbf{B}_i} \boldsymbol{\psi}_{g_r}\right) \mathbf{A}_r + \frac{\partial f_r}{\partial \mathbf{A}_i}, \\
\frac{df_i}{d\mathbf{A}_i} &= -\left(\frac{\partial \mathbf{r}_{g_i}^\top}{\partial \mathbf{B}_r} \boldsymbol{\psi}_{g_i}\right) \mathbf{A}_i - \left(\frac{\partial \mathbf{r}_{g_i}^\top}{\partial \mathbf{B}_r} \boldsymbol{\psi}_{g_i}\right)^\top \mathbf{A}_i - \left(\frac{\partial \mathbf{r}_{g_i}^\top}{\partial \mathbf{B}_i} \boldsymbol{\psi}_{g_i}\right)^\top \mathbf{A}_r \\
&\quad + \left(\frac{\partial \mathbf{r}_{g_i}^\top}{\partial \mathbf{B}_i} \boldsymbol{\psi}_{g_i}\right) \mathbf{A}_r + \frac{\partial f_i}{\partial \mathbf{A}_i},
\end{aligned} \tag{20}$$

. where the last terms in each equation in partial derivative are from the contribution of \mathbf{A} leading to direct dependencies on it.

As a note to the readers, the derivative expression in Eq. (20) above and many such forthcoming equations involve matrices such as $(\partial \mathbf{r}_{g_r} / \partial \mathbf{B}_r)^\top \boldsymbol{\psi}_{g_r}$, which includes complicated tensor-vector products and these can become cumbersome to track and compute. To simplify this, we assume the derivative is calculated after flattening the matrices into vectors. Once the computation is complete, the resulting vectors are reshaped back to their original matrix dimensions. The vector flattening and tensor-vector product is elaborated in detail in Appendix C.

Next, consider the objective function $f = f(\mathbf{u}, \mathbf{v}, \sigma, \mathbf{A})$. Using the governing equation Eq. (8), \mathbf{u} can be expressed as $\mathbf{A}\mathbf{v}/\sigma$, then we have that $f(\mathbf{u}, \mathbf{v}, \sigma, \mathbf{A}) = f(\mathbf{u}, \mathbf{v}(\mathbf{u}, \sigma, \mathbf{A}), \sigma, \mathbf{A})$. If that is done, then the objective function $f = g(\mathbf{u}, \sigma, \mathbf{A})$ as shown above. The same formula in Eq. (20) can be used to compute the derivative of f with respect to \mathbf{A} . This saves the computational effort if \mathbf{A} is very tall.

Since the function f can be any function of $f = f(\mathbf{u}, \mathbf{v}, \sigma, \mathbf{A})$, there

is no general formula that can be devised for that direct contribution of \mathbf{A} . However, if the only direct contribution of \mathbf{A} is from changing of \mathbf{v} to $\mathbf{A}^*\mathbf{u}/\sigma$, then the complex partial derivative components of $\partial f/\partial\mathbf{A}$ can be written in RAD form shown in Appendix D.

It is a fact that the last terms of partial derivatives of $\partial f/\partial\mathbf{A}$ in Eq. (20) can also be obtained by perturbing only \mathbf{A} in the objective function if present, either using FD or automatic differentiation tools such as JAX [62]. These partial derivative terms in Eq. (20) reduce to zero if f is strictly a function of \mathbf{u} and σ .

3.2.2. Adjoint equation of RGMM

We found the adjoint equation for the function $h = f(\mathbf{v}, \sigma, \mathbf{A})$ to be

$$\mathbf{M}_h^\top \boldsymbol{\psi}_h = \frac{\partial h^\top}{\partial \mathbf{w}}, \quad (21)$$

where \mathbf{M}_h is

$$\mathbf{M}_h = \begin{bmatrix} \mathbf{C}_r - \lambda_r \mathbf{I} & -\mathbf{C}_i + \lambda_i \mathbf{I} & -\mathbf{v}_r & \mathbf{v}_i \\ \mathbf{C}_i - \lambda_i \mathbf{I} & \mathbf{C}_r + \lambda_r \mathbf{I} & -\mathbf{v}_i & -\mathbf{v}_r \\ 2\mathbf{v}_r^\top & 2\mathbf{v}_i^\top & 0 & 0 \\ 0 & \mathbf{e}_k^\top & 0 & 0 \end{bmatrix}, \quad (22)$$

and $\boldsymbol{\psi}_h$ is

$$\boldsymbol{\psi}_h = \begin{bmatrix} \boldsymbol{\psi}_{h,r} \\ \boldsymbol{\psi}_{h,i} \\ \boldsymbol{\psi}_{m,h} \\ \boldsymbol{\psi}_{p,h} \end{bmatrix}, \quad (23)$$

where h can be the real (h_r) or imaginary part (h_i) of h if it is complex.

Note that λ which is the eigenvalue is the same in both Eqs. (16) and (21) because both the matrices \mathbf{B} and \mathbf{C} will have some common eigenvalues and λ is one of them. ($\sigma = \sqrt{\lambda}$). The system of equations can be solved by a linear solver such as the solver `numpy.linalg.solve` in Python [63]. Details on this are shed in He et al [42].

We now have two adjoint vectors, namely: $\boldsymbol{\psi}_{h_r}$ and $\boldsymbol{\psi}_{h_i}$ for the function h , each with its real and imaginary parts. The derivative of the residual

vector \mathbf{r} for the function h with respect to the matrix \mathbf{C} is

$$\begin{aligned}
\frac{\partial \mathbf{r}_{h_r}^\top}{\partial \mathbf{C}_r} \boldsymbol{\psi}_{h_r} &= \boldsymbol{\psi}_{h_r, r} \mathbf{v}_r^\top + \boldsymbol{\psi}_{h_r, i} \mathbf{v}_i^\top, \\
\frac{\partial \mathbf{r}_{h_r}^\top}{\partial \mathbf{C}_i} \boldsymbol{\psi}_{h_r} &= -\boldsymbol{\psi}_{h_r, r} \mathbf{v}_i^\top + \boldsymbol{\psi}_{h_r, i} \mathbf{v}_r^\top, \\
\frac{\partial \mathbf{r}_{h_i}^\top}{\partial \mathbf{C}_r} \boldsymbol{\psi}_{h_i} &= \boldsymbol{\psi}_{h_i, r} \mathbf{v}_r^\top + \boldsymbol{\psi}_{h_i, i} \mathbf{v}_i^\top, \\
\frac{\partial \mathbf{r}_{h_i}^\top}{\partial \mathbf{C}_i} \boldsymbol{\psi}_{h_i} &= -\boldsymbol{\psi}_{h_i, r} \mathbf{v}_i^\top + \boldsymbol{\psi}_{h_i, i} \mathbf{v}_r^\top.
\end{aligned} \tag{24}$$

To proceed to the derivative with respect to the matrix \mathbf{A} , we apply chain rule via the reverse automatic differentiation formula (See Appendix B for derivation). Thus, to compute the derivatives of the function $f = h$ with respect to matrix \mathbf{A} , we have

$$\begin{aligned}
\frac{df_r}{d\mathbf{A}_r} &= -\mathbf{A}_r \left(\frac{\partial \mathbf{r}_{h_r}^\top}{\partial \mathbf{C}_r} \boldsymbol{\psi}_{h_r} \right)^\top - \mathbf{A}_r \left(\frac{\partial \mathbf{r}_{h_r}^\top}{\partial \mathbf{C}_r} \boldsymbol{\psi}_{h_r} \right) - \mathbf{A}_i \left(\frac{\partial \mathbf{r}_{h_r}^\top}{\partial \mathbf{C}_i} \boldsymbol{\psi}_{h_r} \right)^\top \\
&\quad + \mathbf{A}_i \left(\frac{\partial \mathbf{r}_{h_r}^\top}{\partial \mathbf{C}_i} \boldsymbol{\psi}_{h_r} \right) + \frac{\partial f_r}{\partial \mathbf{A}_r}, \\
\frac{df_i}{d\mathbf{A}_r} &= -\mathbf{A}_r \left(\frac{\partial \mathbf{r}_{h_i}^\top}{\partial \mathbf{C}_r} \boldsymbol{\psi}_{h_i} \right)^\top - \mathbf{A}_r \left(\frac{\partial \mathbf{r}_{h_i}^\top}{\partial \mathbf{C}_r} \boldsymbol{\psi}_{h_i} \right) - \mathbf{A}_i \left(\frac{\partial \mathbf{r}_{h_i}^\top}{\partial \mathbf{C}_i} \boldsymbol{\psi}_{h_i} \right)^\top \\
&\quad + \mathbf{A}_i \left(\frac{\partial \mathbf{r}_{h_i}^\top}{\partial \mathbf{C}_i} \boldsymbol{\psi}_{h_i} \right) + \frac{\partial f_i}{\partial \mathbf{A}_r}, \\
\frac{df_r}{d\mathbf{A}_i} &= -\mathbf{A}_i \left(\frac{\partial \mathbf{r}_{h_r}^\top}{\partial \mathbf{C}_r} \boldsymbol{\psi}_{h_r} \right)^\top - \mathbf{A}_i \left(\frac{\partial \mathbf{r}_{h_r}^\top}{\partial \mathbf{C}_r} \boldsymbol{\psi}_{h_r} \right) - \mathbf{A}_r \left(\frac{\partial \mathbf{r}_{h_r}^\top}{\partial \mathbf{C}_i} \boldsymbol{\psi}_{h_r} \right)^\top \\
&\quad + \mathbf{A}_r \left(\frac{\partial \mathbf{r}_{h_r}^\top}{\partial \mathbf{C}_i} \boldsymbol{\psi}_{h_r} \right) + \frac{\partial f_r}{\partial \mathbf{A}_i}, \\
\frac{df_i}{d\mathbf{A}_i} &= -\mathbf{A}_i \left(\frac{\partial \mathbf{r}_{h_i}^\top}{\partial \mathbf{C}_r} \boldsymbol{\psi}_{h_i} \right)^\top - \mathbf{A}_i \left(\frac{\partial \mathbf{r}_{h_i}^\top}{\partial \mathbf{C}_r} \boldsymbol{\psi}_{h_i} \right) - \mathbf{A}_r \left(\frac{\partial \mathbf{r}_{h_i}^\top}{\partial \mathbf{C}_i} \boldsymbol{\psi}_{h_i} \right)^\top \\
&\quad + \mathbf{A}_r \left(\frac{\partial \mathbf{r}_{h_i}^\top}{\partial \mathbf{C}_i} \boldsymbol{\psi}_{h_i} \right) + \frac{\partial f_i}{\partial \mathbf{A}_i},
\end{aligned} \tag{25}$$

where the last terms in each equation in partial derivative are from the contribution of \mathbf{A} leading to direct dependencies on it.

Consider the objective function $f = f(\mathbf{u}, \mathbf{v}, \sigma, \mathbf{A})$. Using the govern-

ing equation Eq. (8), \mathbf{u} can be expressed as $\mathbf{A}\mathbf{v}/\sigma$, then we have that $f(\mathbf{u}, \mathbf{v}, \sigma, \mathbf{A}) = f(\mathbf{u}(\mathbf{v}, \sigma, \mathbf{A}), \mathbf{v}, \sigma, \mathbf{A})$. If that is done, then the objective function $f = h(\mathbf{v}, \sigma, \mathbf{A})$ as shown above. The same formula in Eq. (25) can be used to compute the derivative of f with respect to \mathbf{A} . This saves the computational effort if \mathbf{A} is very wide.

Since the function f can be any function of $f = f(\mathbf{u}, \mathbf{v}, \sigma, \mathbf{A})$, there is no general formula that can be devised for that direct contribution of \mathbf{A} . However, if the only direct contribution of \mathbf{A} is from changing of \mathbf{u} to $\mathbf{A}\mathbf{v}/\sigma$, then the complex partial derivative components of $\partial f/\partial \mathbf{A}$ can be written in RAD form shown in Appendix D.

It is a fact that the last terms of partial derivatives of $\partial f/\partial \mathbf{A}$ in Eq. (20) can also be obtained by perturbing only \mathbf{A} in the objective function if present, either using FD or automatic differentiation tools such as JAX [62]. These partial derivative terms in Eq. (20) reduce to zero if f is strictly a function of \mathbf{u} and σ .

To summarize keeping the minimization of computational effort in mind, we employ Eqs. (16) to (18) and (20) if the function is expressed in terms of the singular variables \mathbf{u} and σ . If it is expressed in terms of \mathbf{v} and σ , then we use Eqs. (21) to (23) and (25).

3.3. Adjoint equation of SEMM

In this section, we directly apply the adjoint method to the SVD governing equations as listed in the preceding section Section 2. We found the adjoint equation for the function, f , to be

$$\mathbf{M}_f^\top \boldsymbol{\psi}_f = \frac{\partial f}{\partial \mathbf{w}}^\top, \quad (26)$$

where \mathbf{J} is the Jacobian of function f with respect to the state variables vector \mathbf{w} ($\partial f/\partial \mathbf{w}$), \mathbf{M}_f and $\boldsymbol{\psi}_f$ are

$$\mathbf{M}_f = \begin{bmatrix} -\sigma_r \mathbf{I} & \sigma_i \mathbf{I} & \mathbf{A}_r & -\mathbf{A}_i & -\mathbf{u}_r & \mathbf{u}_i \\ -\sigma_i \mathbf{I} & -\sigma_r \mathbf{I} & \mathbf{A}_i & \mathbf{A}_r & -\mathbf{u}_i & -\mathbf{u}_r \\ \mathbf{A}_r^\top & \mathbf{A}_i^\top & -\sigma_r \mathbf{I} & \sigma_i \mathbf{I} & -\mathbf{v}_r & \mathbf{v}_i \\ -\mathbf{A}_i^\top & \mathbf{A}_r^\top & -\sigma_i \mathbf{I} & -\sigma_r \mathbf{I} & -\mathbf{v}_i & -\mathbf{v}_r \\ 2\mathbf{u}_r^\top & 2\mathbf{u}_i^\top & \mathbf{0} & \mathbf{0} & 0 & 0 \\ \mathbf{0} & \mathbf{e}_k^\top & \mathbf{0} & \mathbf{0} & 0 & 0 \end{bmatrix}, \quad \boldsymbol{\psi}_f = \begin{bmatrix} \psi_{v_r} \\ \psi_{v_i} \\ \psi_{u_r} \\ \psi_{u_i} \\ \psi_m \\ \psi_p \end{bmatrix}. \quad (27)$$

Here, m and p represent the magnitude and phase respectively. The partial derivatives of f_r and f_i with respect to \mathbf{A}_r and \mathbf{A}_i are then

$$\begin{aligned}
\frac{df_r}{d\mathbf{A}_r} &= -\frac{\partial \mathbf{r}}{\partial \mathbf{A}_r}^\top \boldsymbol{\psi}_r + \frac{\partial f_r}{\partial \mathbf{A}_r}, \\
\frac{df_r}{d\mathbf{A}_i} &= -\frac{\partial \mathbf{r}}{\partial \mathbf{A}_i}^\top \boldsymbol{\psi}_r + \frac{\partial f_r}{\partial \mathbf{A}_i}, \\
\frac{df_i}{d\mathbf{A}_r} &= -\frac{\partial \mathbf{r}}{\partial \mathbf{A}_r}^\top \boldsymbol{\psi}_i + \frac{\partial f_i}{\partial \mathbf{A}_r}, \\
\frac{df_i}{d\mathbf{A}_i} &= -\frac{\partial \mathbf{r}}{\partial \mathbf{A}_i}^\top \boldsymbol{\psi}_i + \frac{\partial f_i}{\partial \mathbf{A}_i}.
\end{aligned} \tag{28}$$

The $(\partial \mathbf{r} / \partial \mathbf{A})^\top \boldsymbol{\psi}$ terms in the RHS of the equations above are (derivation in Appendix E)

$$\begin{aligned}
\frac{\partial \mathbf{r}}{\partial \mathbf{A}_r}^\top \boldsymbol{\psi} &= \boldsymbol{\psi}_{v_r} \mathbf{v}_r^\top + \boldsymbol{\psi}_{v_i} \mathbf{v}_i^\top + \mathbf{u}_r \boldsymbol{\psi}_{u_r}^\top + \mathbf{u}_i \boldsymbol{\psi}_{u_i}^\top, \\
\frac{\partial \mathbf{r}}{\partial \mathbf{A}_i}^\top \boldsymbol{\psi} &= -\boldsymbol{\psi}_{v_r} \mathbf{v}_i^\top + \boldsymbol{\psi}_{v_i} \mathbf{v}_r^\top + \mathbf{u}_i \boldsymbol{\psi}_{u_r}^\top - \mathbf{u}_r \boldsymbol{\psi}_{u_i}^\top,
\end{aligned} \tag{29}$$

where $\boldsymbol{\psi} = \boldsymbol{\psi}_r$ from Eq. (28) if $f = f_r$ in Eq. (27). Similarly, $\boldsymbol{\psi} = \boldsymbol{\psi}_i$ from Eq. (28) if $f = f_i$ in Eq. (27).

3.4. RAD method for singular value derivative

The technique described so far can compute derivatives of the singular variables at once, in any combination. If the derivative of just the dominant singular value is sought, we propose the following RAD based formulae: (Derivation in Appendix F).

$$\begin{aligned}
\frac{d\sigma}{d\mathbf{A}_r} &= \mathbf{u}_r \mathbf{v}_r^\top + \mathbf{u}_i \mathbf{v}_i^\top, \\
\frac{d\sigma}{d\mathbf{A}_i} &= -\mathbf{u}_r \mathbf{v}_i^\top + \mathbf{u}_i \mathbf{v}_r^\top.
\end{aligned} \tag{30}$$

For the purely real case if $\mathbf{A} = \mathbf{A}_r$, it is

$$\frac{d\sigma}{d\mathbf{A}} = \mathbf{u} \mathbf{v}^\top, \tag{31}$$

where $\mathbf{u} \in \mathbb{R}, \mathbf{v} \in \mathbb{R}$ and $\mathbf{A} \in \mathbb{R}$. Further, the formula in Eq. (30) reduces to Eq. (31) if the imaginary parts are set to zero.

4. Numerical results

In this section, we verify the proposed adjoint-based method via the GMM and SEMM using two complex-valued matrices, one square matrix and one tall rectangular matrix by comparing the values of the obtained derivatives with the values obtained from FD. The tall rectangular matrix means that it has number of rows greater than the number of columns here [34]. The square matrix is taken and the derivative results from adjoint method for LGMM, RGMM, SEMM and the singular value derivative RAD formula are compared with the results from the FD computation in Section 4.1 for a randomly selected objective function. This is repeated for the rectangular matrix in Section 4.2.

Finally, to show scalability, we compute the singular value derivatives of the singular values from the proper orthogonal decomposition (POD) through SVD of a large dataset of transition to turbulence of flow over a flat plate in Section 4.3. The data was sourced from the JHTDB and the POD was performed by the method of snapshots.

4.1. Square matrix derivative computation

The randomly selected square matrix is

$$\mathbf{A} = \mathbf{A}_r + i\mathbf{A}_i = \begin{bmatrix} -1.01 & 0.86 & -31.42 \\ 3.98 & 0.53 & -7.04 \\ 3.3 & 8.26 & -3.89 \end{bmatrix} + i \begin{bmatrix} 0.6 & 0.79 & 5.47 \\ 7.21 & 1.9 & 0.58 \\ 3.42 & 8.97 & 0.3 \end{bmatrix}. \quad (32)$$

It was ensured that no repeated eigenvalues were found in the eigen-decompositions of $\mathbf{B} = \mathbf{A}\mathbf{A}^*$ and $\mathbf{C} = \mathbf{A}^*\mathbf{A}$. The dominant singular value and its respective left and right singular vectors are

$$\begin{aligned} \sigma_1 &= 33.16357940928816, \\ \mathbf{u}_r + i\mathbf{u}_i &= \begin{bmatrix} 0.9572042 \\ 0.23641926 \\ 0.16616206 \end{bmatrix} + i \begin{bmatrix} 0 \\ 0.01549572 \\ 0.00401452 \end{bmatrix}, \\ \mathbf{v}_r + i\mathbf{v}_i &= \begin{bmatrix} -0.00513976 \\ -0.05740808 \\ 0.99047735 \end{bmatrix} + i \begin{bmatrix} 0.08569246 \\ 0.09104565 \\ 0 \end{bmatrix}. \end{aligned} \quad (33)$$

The objective function was chosen as

$$f = \mathbf{c}_u^T \mathbf{u} + \mathbf{c}_v^T \mathbf{v} + c_\sigma \sigma + c_A \text{Tr}(\mathbf{A}), \quad (34)$$

where $\text{Tr}(\cdot)$ is the trace operator and the constants were

$$\mathbf{c}_u = \mathbf{c}_v = \begin{bmatrix} 0.16 + 0.78i \\ 0.53 + 0.11i \\ 0.11 + 0.77i \end{bmatrix}, \quad (35)$$

$$c_\sigma = c_A = 1,$$

where the constants were randomly selected.

In Section 3.2, we showed two ways to compute the derivative. One is to express \mathbf{u} in terms of $\mathbf{v}, \sigma, \mathbf{A}$ which is the LGMM or to express \mathbf{v} in terms of $\mathbf{u}, \sigma, \mathbf{A}$ which is the RGMM. If \mathbf{v} is expressed in terms of $\mathbf{u}, \sigma, \mathbf{A}$ following the governing equation in Eq. (8), the objective function in Eq. (34) becomes

$$f = \mathbf{c}_u^T \mathbf{u} + \mathbf{c}_v^T \frac{\mathbf{A}^* \mathbf{u}}{\sigma} + c_\sigma \sigma + c_A \text{Tr}(\mathbf{A}). \quad (36)$$

Similarly if \mathbf{u} is expressed in terms of $\mathbf{v}, \sigma, \mathbf{A}$, the objective function in Eq. (34) becomes

$$f = \mathbf{c}_u^T \frac{\mathbf{A} \mathbf{v}}{\sigma} + \mathbf{c}_v^T \mathbf{v} + c_\sigma \sigma + c_A \text{Tr}(\mathbf{A}). \quad (37)$$

Thus, we have reduced the function from $f(\mathbf{u}, \mathbf{v}, \sigma, \mathbf{A})$ to either $f(\mathbf{u}, \sigma, \mathbf{A})$ for LGMM or $f(\mathbf{v}, \sigma, \mathbf{A})$ for RGMM derivative computation.

For the LGMM, we apply Eqs. (16) to (18) and (20) to compute the derivative of f with respect to matrix \mathbf{A} . For the RGMM, we use Eqs. (21) to (23) and (25). For the Eq. (21) and Eq. (16), the Jacobian \mathbf{J} can be computed analytically, but for the general case, this becomes cumbersome to implement each time the objective function changes. Thus, the automatic differentiation tool JAX [62] was employed for the Jacobian of the function with respect to the state variables. This was also done for the direct contribution of matrix \mathbf{A} , as shown in the objective function Eq. (34), for the partial derivatives in Eqs. (20) and (25). Thus, the procedure of using JAX [62] for the Jacobian and direct contribution of matrix \mathbf{A} is elaborated in Appendix G. Results from this derivative computation are shown in Table 2.

Next, the same function and matrix were taken (Eqs. (32) and (34)) and used in the SEMM approach shown in Section 3.3. The Eqs. (26) to (29) were used to compute the derivative. Once again, JAX [62] was used for evaluation of the Jacobian in Eq. (26) and for the partial derivatives of $\partial f/\partial \mathbf{A}$ in Eq. (28) (See Appendix G). Results from this derivative computation are shown in Table 2.

The LGMM, RGMM, and SEMM derivatives were obtained for the same objective function and square matrix and, therefore, matched with each other. If the objective function f is $f = \sigma$, which is done by setting the other constants to zero and constant $c_\sigma = 1$ in Eq. (34), then the RAD formula Eq. (30) can be used to compute the derivative. Results from this derivative computation are shown in Table 4 for the square matrix \mathbf{A} (Eq. (32)). To further establish confidence in the proposed methodology and results, a comparison between the obtained derivative results was made against the results from FD computations (Described in Appendix H), which matched too, as seen in Table 2.

4.2. Rectangular matrix derivative computation

Consider the tall complex matrix \mathbf{A} as

$$\mathbf{A}_r + i\mathbf{A}_i = \begin{bmatrix} 6.3 & 5 \\ -5.35 & 0.62 \\ -7.49 & -1.6 \\ -0.15 & 0.71 \end{bmatrix} + i \begin{bmatrix} 4.49 & -9.95 \\ -1.23 & 7.29 \\ 6.17 & -1.9 \\ -4.89 & -3.63 \end{bmatrix}, \quad (38)$$

and the chosen singular variables are

$$\begin{aligned} \sigma &= 17.275386033399094, \\ \mathbf{u}_r + i\mathbf{u}_i &= \begin{bmatrix} -0.64373688 \\ 0.51599116 \\ 0.2346775 \\ -0.13537246 \end{bmatrix} + i \begin{bmatrix} -0.41836418 \\ 0.05007437 \\ -0.20205518 \\ 0.16611561 \end{bmatrix}, \\ \mathbf{v}_r + i\mathbf{v}_i &= \begin{bmatrix} -0.72661509 \\ 0.05431442 \end{bmatrix} + i \begin{bmatrix} 0 \\ -0.68489449 \end{bmatrix}. \end{aligned} \quad (39)$$

The objective function was taken to be same as in Eq. (34) and the constants were the same as well (Eq. (35)), except for \mathbf{c}_u and \mathbf{c}_v which were chosen to

be

$$\mathbf{c}_u = \begin{bmatrix} 0.12 + 0.67i \\ 0.56 + 3.67i \\ 0.46 + 2.96i \\ 2.89 + 1.48i \end{bmatrix}, \quad \mathbf{c}_v = \begin{bmatrix} 7.12 + 0.97i \\ 0.26 + 6.47i \end{bmatrix}. \quad (40)$$

Once again, these constants were randomly selected. The constants \mathbf{c}_u and \mathbf{c}_v for the rectangular matrix were chosen differently because they must adhere to the shape of the vectors \mathbf{u} and \mathbf{v} .

The same process as in Section 4.1 was followed for the derivative computation of each of the routes: LGMM, RGMM and SEMM, and the results were compared with FD. The results are tabulated in Table 3.

If the objective function f is $f = \sigma$, which is done by setting the other constants to zero and constant $c_\sigma = 1$ in Eq. (34), then the RAD formula Eq. (30) can be employed. Results from this derivative computation are shown in Table 5 for the rectangular matrix \mathbf{A} (Eq. (38)).

Table 4: Verification of the RAD formula for singular value derivative with FD for the square matrix

Type	Index	RAD	FD
$d\sigma/d\mathbf{A}_r$	(1, 1)	0.018703061899253	0.018702181137087
$d\sigma/d\mathbf{A}_r$	(1, 2)	0.068881276214858	0.068880360970525
$d\sigma/d\mathbf{A}_r$	(1, 3)	-0.934470093986586	-0.934470051561220
$d\sigma/d\mathbf{A}_i$	(1, 1)	0.080015153716675	0.080016050674203
$d\sigma/d\mathbf{A}_i$	(1, 2)	0.076615998520789	0.076616849753464
$d\sigma/d\mathbf{A}_i$	(1, 3)	0.160118791389606	0.160120613657000

Table 5: Verification of the RAD formula for singular value derivative with FD for the rectangular matrix

Type	Index	RAD	FD
$d\sigma/d\mathbf{A}_r$	(1, 1)	0.467749108787955	0.467748947130531
$d\sigma/d\mathbf{A}_r$	(1, 2)	0.251572392322310	0.251571147913410
$d\sigma/d\mathbf{A}_i$	(1, 1)	0.303989439817427	0.303989750705114
$d\sigma/d\mathbf{A}_i$	(1, 2)	-0.463615299320613	-0.463615023704733

Table 2: Verification of the adjoint derivatives with FD for square matrix case

Type	Index	Adjoint LGMM	Adjoint RGMM	Adjoint SEMM	FD
$df_r/d\mathbf{A}_r$	(1, 1)	1.006352961803713	1.006352961803713	1.006352961803713	1.006352068344540
$df_r/d\mathbf{A}_r$	(1, 2)	0.043276271008604	0.043276271008604	0.043276271008604	0.043275413474930
$df_r/d\mathbf{A}_r$	(1, 3)	-0.936930641525170	-0.936930641525170	-0.936930641525170	-0.936930476314046
$df_r/d\mathbf{A}_i$	(1, 1)	0.063695888970744	0.063695888970744	0.063695888970744	0.063696809604608
$df_r/d\mathbf{A}_i$	(1, 2)	0.082766443637231	0.082766443637231	0.082766443637231	0.082767300568776
$df_r/d\mathbf{A}_i$	(1, 3)	0.156944460318835	0.156944460318835	0.156944460318835	0.156946299512128
$df_i/d\mathbf{A}_r$	(1, 1)	-0.017846334274906	-0.017846334274906	-0.017846334274906	-0.017846180533354
$df_i/d\mathbf{A}_r$	(1, 2)	0.002833157022766	0.002833157022766	0.002833157022766	0.002833298928806
$df_i/d\mathbf{A}_r$	(1, 3)	0.006354411136774	0.006354411136774	0.006354411136774	0.006354630599503
$df_i/d\mathbf{A}_i$	(1, 1)	1.006719107202561	1.006719107202561	1.006719107202561	1.006719100082876
$df_i/d\mathbf{A}_i$	(1, 2)	0.019954391307143	0.019954391307143	0.019954391307143	0.019954295993330
$df_i/d\mathbf{A}_i$	(1, 3)	0.003910503966226	0.003910503966226	0.003910503966226	0.003910511914285

Table 3: Verification of the adjoint derivatives with FD for rectangular matrix case

Type	Index	Adjoint LGMM	Adjoint RGMM	Adjoint SDMM	FD
$df_r/d\mathbf{A}_r$	(1, 1)	1.846102900714162	1.846102900714162	1.846102900714162	1.846101064018058
$df_r/d\mathbf{A}_r$	(1, 2)	-0.006821647620363	-0.006821647620363	-0.006821647620363	-0.006822084230862
$df_r/d\mathbf{A}_i$	(1, 1)	0.354647919899091	0.354647919899091	0.354647919899091	0.354647895051130
$df_r/d\mathbf{A}_i$	(1, 2)	-0.124582311966832	-0.124582311966832	-0.124582311966832	-0.124581340799068
$df_i/d\mathbf{A}_r$	(1, 1)	0.227870193134751	0.227870193134751	0.227870193134751	0.227870147639919
$df_i/d\mathbf{A}_r$	(1, 2)	0.353104252473483	0.353104252473483	0.353104252473483	0.353103555283951
$df_i/d\mathbf{A}_i$	(1, 1)	0.780271281223158	0.780271281223158	0.780271281223158	0.780273927247777
$df_i/d\mathbf{A}_i$	(1, 2)	0.113513089065063	0.113513089065063	0.113513089065063	0.113512610866451

4.3. Large dataset derivative computation

In this section, we compute the derivative of the first six singular values from the proper orthogonal decomposition of the fluid flow over a flat plate. This flow is transitioning from laminar to turbulent regime and is sourced from JHTDB [60]. We use the RAD based singular value derivative for the real-valued case Eq. (31) on the JHTDB dataset.

4.3.1. Dataset description

The laminar–turbulent transitional flow dataset from JHTB was used in this study [60]. This data-set was produced from direct numerical simulation of incompressible flow of fluid over a flat plate in a developing boundary layer. The flat plate was given a leading edge and the Reynolds number $Re = 800$, where $Re = U_\infty L/\nu$. Here, $U_\infty = 1$ is the non-dimensional free stream velocity, $L = 1$ is the length scale set to half-plate thickness and $\nu = 1.24 \times 10^{-3}$ is the kinematic viscosity.

The dataset is a rectangular domain in 3D with set of grid points in cartesian coordinates (x, y, z) , each having the state variables of x -component of velocity u , y -component of velocity v , z -component of velocity w and the pressure P . All values in the database are non-dimensionalized. The database domain is from $[30.2185L, 1000L]$ in the x direction, $[0, 26.48L]$ in the y direction and $[0, 240L]$ in the z direction. The cutout was taken from $[100L, 600L]$ in the x direction, $[0, 10L]$ in the y direction and $[80L, 120L]$ in the z direction, which resulted in a domain size of $(500L \times 10L \times 40L)$. The number of grid points in the cutout was $n_x \times n_y \times n_z = 1712 \times 85 \times 342$. Here n_x, n_y and n_z are the number of grid points in the x, y and z directions, respectively. Thus, there are $m_0 = 1712 \times 85 \times 342 = 49.76784 \times 10^6$ spatial points. The cutout time stored is $\bar{t} \in [1000, 1175]$ where $\bar{t} = L/U_\infty$ is the non-dimensional time. Thus, there were 75 time-steps stored, with each step having a physical time of $\delta\bar{t} = 0.25$ giving a total physical time, \bar{t} , equal to $75 \times 0.25 = 18.75$. The last 75 time steps were chosen after studying the flow field carefully and ensuring a statistically stationary state, where by stationary we mean the transition location. Further details on the grid and velocity data, the turbulence characteristics and other flow related data can be found at JHTDB [60].

4.3.2. POD and its relationship with SVD

POD of the obtained data cutout was performed on the velocity data. Thus, there are $m = n_x \times n_y \times n_z \times 3 = m_0 \times 3 = 149.30352 \times 10^6$ states

for each time step. In POD, the time-series data is arranged into a snapshot matrix $\mathbf{X} \in \mathbb{R}^{m \times n}$ where m is the number of states arranged in a vectorized form for each time step and n equals to the number of time-steps or snapshots of the data. SVD on this snapshot matrix is performed to obtain the modes, their energies and their temporal coefficients. In the current study, since velocity data was used for the POD, the matrix \mathbf{X} is defined as

$$\mathbf{X} = \begin{bmatrix} u_{1,1} & u_{1,2} & \cdots & u_{1,n} \\ u_{2,1} & u_{2,2} & \cdots & u_{2,n} \\ \vdots & \vdots & \vdots & \vdots \\ u_{m_0,1} & u_{m_0,2} & \cdots & u_{m_0,n} \\ \hline v_{1,1} & v_{1,2} & \cdots & v_{1,n} \\ v_{2,1} & v_{2,2} & \cdots & v_{2,n} \\ \vdots & \vdots & \vdots & \vdots \\ v_{m_0,1} & v_{m_0,2} & \cdots & v_{m_0,n} \\ \hline w_{1,1} & w_{1,2} & \cdots & w_{1,n} \\ w_{2,1} & w_{2,2} & \cdots & w_{2,n} \\ \vdots & \vdots & \vdots & \vdots \\ w_{m_0,1} & w_{m_0,2} & \cdots & w_{m_0,n} \end{bmatrix}, \quad (41)$$

where $u_{i,k}$ is the x -directional velocity at the i^{th} grid point and k^{th} time-step; similar for $v_{i,k}$ and $w_{i,k}$. The number of time-steps is $n = 20$ as mentioned earlier. Instead of conducting POD on the original dataset, it is recommended to instead conduct the POD with respect to the perturbed state [32]. The perturbed snapshot matrix is defined as

$$\mathbf{X}' = \mathbf{X} - \frac{1}{n} \mathbf{X} \mathbf{1}_n \mathbf{1}_n^T, \quad (42)$$

where $\mathbf{X}' \in \mathbb{R}^{m \times n}$ is the perturbed snapshots matrix, and $\mathbf{1}_n \in \mathbb{R}^n$ is a vector of ones with dimension n . SVD is then performed on this matrix \mathbf{X}' which yields

$$\mathbf{X}' = \mathbf{\Phi} \mathbf{\Sigma} \mathbf{\Psi}^T, \quad (43)$$

where $\mathbf{\Phi} \in \mathbb{R}^{m \times m}$, $\mathbf{\Sigma} \in \mathbb{R}^{m \times n}$, and $\mathbf{\Psi} \in \mathbb{R}^{n \times n}$. Columns of $\mathbf{\Phi}$ contain the POD modes, $\mathbf{\Sigma}$ is the rectangular matrix with singular values on the main

diagonal and zeros elsewhere, and each of these values contains the energy associated with the corresponding mode. The POD was performed through the method of snapshots (See Appendix I) that gave the singular values and vectors as it is an efficient way to perform POD [32].

4.3.3. POD derivative results

The results of the POD computations along with the full order model (FOM) are shown in Fig. 1. The first, third and sixth modes are shown for sake of compactness and representation, although all of the modes were captured in the computations. The velocity data was visualized using the Q -criterion with Q -2 iso-surfaces of 0.001 in magnitude and colored by the u -velocity magnitude of the FOM flow field [64]. The Q -criterion identifies vortices as regions where the rotation rate dominates over the strain rate. It is defined as

$$Q = \frac{1}{2} (||\boldsymbol{\Omega}||^2 - ||\mathbf{S}||^2), \quad (44)$$

where Q is the Q -criterion value, $\boldsymbol{\Omega}$ is the antisymmetric rotation tensor, \mathbf{S} is the symmetric strain-rate tensor, $||\boldsymbol{\Omega}||^2$ is the squared norm of the rotation tensor, and $||\mathbf{S}||^2$ is the squared norm of the strain-rate tensor. These tensors are defined as

$$\mathbf{S} = \frac{1}{2} (\nabla \mathbf{u} + \nabla \mathbf{u}^\top), \quad (45)$$

where \mathbf{u} is the velocity vector containing the x , y and z component of velocities in a vectorized form and $\nabla \mathbf{u}$ is the velocity gradient tensor. The rotation tensor is

$$\boldsymbol{\Omega} = \frac{1}{2} (\nabla \mathbf{u} - \nabla \mathbf{u}^\top). \quad (46)$$

The squared norm $||\cdot||^2$ for the tensors is defined as

$$||\mathbf{S}||^2 = \text{Tr}(\mathbf{S}^\top \mathbf{S}), \quad (47)$$

for the symmetric strain tensor and

$$||\boldsymbol{\Omega}||^2 = \text{Tr}(\boldsymbol{\Omega}^\top \boldsymbol{\Omega}), \quad (48)$$

for the anti-symmetric strain tensor.

In regions where $Q > 0$, the local rotation dominates over strain, and these regions are identified as vortices [64]. The Q iso-surfaces were visualized at iso values of $Q = 0.001$ in Fig. 1. These Q -contours were made at four

selected time values t_1, t_2, t_3, t_4 such that $t_1 < t_2 < t_3 < t_4$. The non-dimensional time values were $t_1 = 1075, t_2 = 1076.5, t_3 = 1078$ and $t_4 = 1080$.

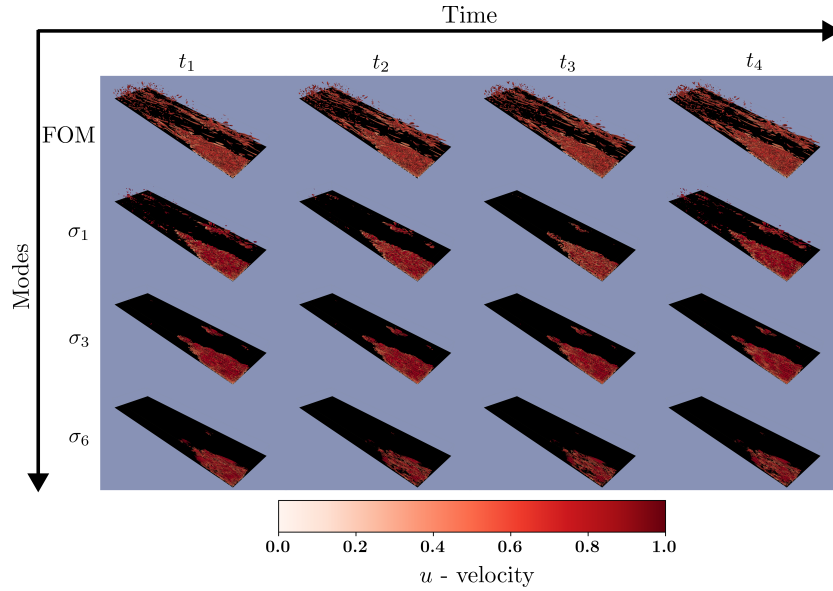


Figure 1: POD modes of the JHTDB transitional boundary layer dataset. Vortical structures are Q iso-surfaces ($Q = 0.001$)

Physically, the derivative computation of the singular values is the measure of how sensitive each singular value is to perturbations in the original snapshot matrix. Thus, we get three directions of derivatives of the velocities as there are three components of the velocity data u, v and w . With

reference to Eq. (41), we can see that

$$\frac{d\sigma_i}{d\mathbf{X}} = \begin{bmatrix} \frac{d\sigma_i}{du_{1,1}} & \frac{d\sigma_i}{du_{1,2}} & \dots & \frac{d\sigma_i}{du_{1,n}} \\ \frac{d\sigma_i}{du_{2,1}} & \frac{d\sigma_i}{du_{2,2}} & \dots & \frac{d\sigma_i}{du_{2,n}} \\ \vdots & \vdots & \vdots & \vdots \\ \frac{d\sigma_i}{du_{m_0,1}} & \frac{d\sigma_i}{du_{m_0,2}} & \dots & \frac{d\sigma_i}{du_{m_0,n}} \\ \hline \frac{d\sigma_i}{dv_{1,1}} & \frac{d\sigma_i}{dv_{1,2}} & \dots & \frac{d\sigma_i}{dv_{1,n}} \\ \frac{d\sigma_i}{dv_{2,1}} & \frac{d\sigma_i}{dv_{2,2}} & \dots & \frac{d\sigma_i}{dv_{2,n}} \\ \vdots & \vdots & \vdots & \vdots \\ \frac{d\sigma_i}{dv_{m_0,1}} & \frac{d\sigma_i}{dv_{m_0,2}} & \dots & \frac{d\sigma_i}{dv_{m_0,n}} \\ \hline \frac{d\sigma_i}{dw_{1,1}} & \frac{d\sigma_i}{dw_{1,2}} & \dots & \frac{d\sigma_i}{dw_{1,n}} \\ \frac{d\sigma_i}{dw_{2,1}} & \frac{d\sigma_i}{dw_{2,2}} & \dots & \frac{d\sigma_i}{dw_{2,n}} \\ \vdots & \vdots & \vdots & \vdots \\ \frac{d\sigma_i}{dw_{m_0,1}} & \frac{d\sigma_i}{dw_{m_0,2}} & \dots & \frac{d\sigma_i}{dw_{m_0,n}} \end{bmatrix}, \quad (49)$$

where $d\sigma/du$ is the derivative of the singular value with respect to the u -velocity. Similarly this holds for $d\sigma/dv$ and $d\sigma/dw$.

From this, it is clear that the singular value derivative is directional in the three dimensional space it is evaluated for through POD. The snapshot matrix had 149.30352×10^6 rows equal to the number of states and 75 columns equal to the number of time steps as aforementioned and the derivatives of the singular value with respect to this snapshot matrix were computed using the RAD formula shown in Eq. (31). Results from this derivative computation are shown in Fig. 2 which showcases the derivatives of the first, third and sixth modes along the x -direction for the first time-step. In this figure, the Q -criterion plot at $Q = 0.001$ for the FOM was made and colored by the singular value derivatives. These Q -contours were again made for four selected time values t_1, t_2, t_3, t_4 such that $t_1 < t_2 < t_3 < t_4$. The non-dimensional time values were $t_1 = 1075, t_2 = 1076.5, t_3 = 1078$ and $t_4 = 1080$. Thus, we have shown the scalability of the proposed RAD-based singular value derivative formula working for a large matrix derived through POD of the flow over flat plate.

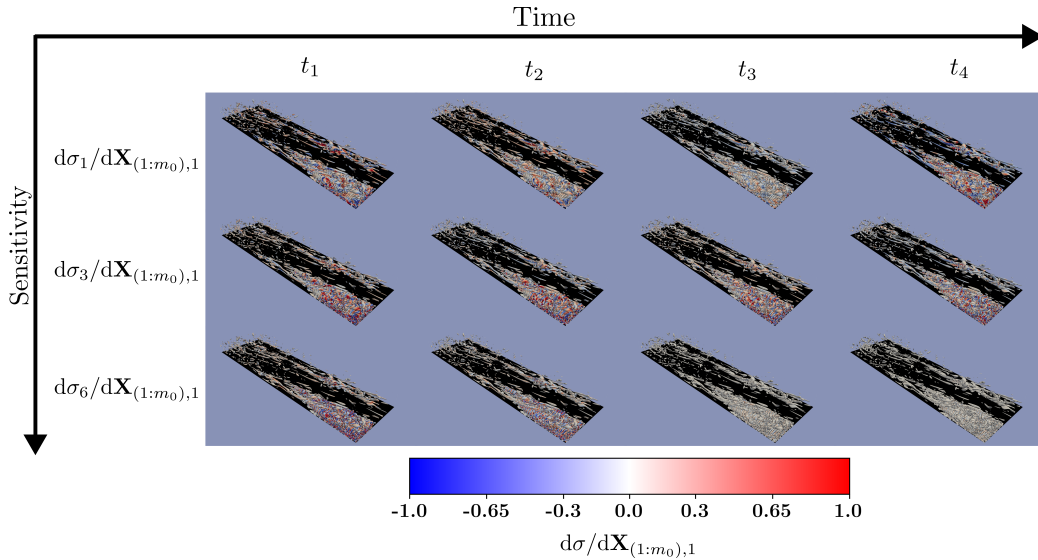


Figure 2: x -direction singular value derivatives of the POD modes of JHTDB transitional boundary layer dataset. Vortical structures are Q iso-surfaces ($Q = 0.001$)

5. Conclusions

In this paper, we developed two adjoint-based methods to compute the singular values and singular vector derivative and an RAD formula to compute the singular value derivative. The proposed differentiable SVD algorithms do not scale with the number of inputs and do not require all of the singular variables during derivative computation, thus reducing the computational cost, they are relatively easier to implement, and are accurately, being implicit analytic in nature of the solution. All the derivative computation strategies proposed in the current manuscript can handle complex-valued inputs and outputs.

We proposed two adjoint method approaches leveraging the relationship between EVP and SVD. In the first approach, we leverage the relationship between the SVD of a matrix and the EVP of its Gram matrices. We call it the Gram matrix method or GMM. In the second approach, we leverage the relationship between the SVD of a matrix and the EVP of its symmetric embedding. We call it the symmetric embedding matrix method or SEMM. The adjoint-based GMM computes the derivative by breaking down the SVD into two eigenvalue problems of the Gram matrices and applies the adjoint

method to the governing equations for each EVP. This results in two formulations, the Left Gram Matrix Method or LGMM and the Right Gram Matrix Method RGMM, deriving their names from the fact that each Gram matrix either yields the left or right singular vectors in their EVP solutions.

The adjoint-based SEMM computes this derivative by directly applying the adjoint method to the SVD governing equations resulting from the symmetric embedding EVP. Each method holds its merits based on the objective function whose derivative is desired and the nature of matrix \mathbf{A} being sparse or dense. If the matrix is dense, the computation of the Gram matrices of the matrix can become costly. To avoid this, the SEMM is used. If the matrix is sparse, the former method, GMM, should be used. If the matrix is square, LGMM or RGMM are both equivalent. If the matrix is tall, LGMM is advised to be used, otherwise, RGMM. Finally, we also proposed a general RAD dot product identity for general complex-valued functions that are complex-differentiable.

The results from derivative computations of two complex matrices, square and rectangular, were compared against the results from FD approximations, and we achieved a 5–6 digit match. An implementation of the real-valued form of the proposed singular value derivative RAD formula was shown by applying the formula on the snapshot matrix of a large cutout of the JHTDB dataset in a 3-dimensional space and obtaining the singular values and vectors through POD. The snapshot matrix had 149.30352×10^6 rows equal to the number of states and 75 columns equal to the number of time steps. There is no limitation set on the objective function under consideration, making the proposed method well-suited to large-scale design optimization problems involving gradients of SVD with respect to several design variables, for instance, in differentiable POD or differentiable resolvent analyses that find applications in various engineering-design optimization problems.

6. Acknowledgement

The first author would like to thank Ariel Lubonja from John Hopkins University for help with the data retrieval process of the JHTDB flat plate boundary layer dataset.

References

- [1] G. Strang, Introduction to Linear Algebra, Sixth Edition, Wellesley-Cambridge Press, Philadelphia, PA, 2022.

doi:10.1137/1.9781733146678.

- [2] C. Eckart, G. Young, A principal axis transformation for non-hermitian matrices (1939).
- [3] E. Candès, B. Recht, Exact matrix completion via convex optimization, *Communications of the ACM* 55 (2012) 111–119. doi:10.1145/2184319.2184343.
- [4] K.-W. Gwak, G. Y. Masada, Structural analysis and optimization of nonlinear control systems using singular value decomposition, *Journal of Dynamic Systems, Measurement, and Control* 127 (2004) 105–113. doi:10.1115/1.1876495.
- [5] M. Khalil, S. Adhikari, A. Sarkar, Linear system identification using proper orthogonal decomposition, *Mechanical Systems and Signal Processing* 21 (2007) 3123–3145. doi:10.1016/j.ymsp.2007.03.007.
- [6] S. Sarkar, A. Dong, J. S. Gero, Design optimization problem reformulation using singular value decomposition, *Journal of Mechanical Design* 131 (2009). doi:10.1115/1.3179148.
- [7] S. d. Lucas Bodas, An optimization method for conceptual design in engineering systems based on high order singular value decomposition, Ph.D. thesis, Universidad Politecnica de Madrid - University Library, 2012. doi:10.20868/upm.thesis.13202.
- [8] X. Zhao, B. Ye, Singular value decomposition packet and its application to extraction of weak fault feature, *Mechanical Systems and Signal Processing* 70–71 (2016) 73–86. doi:10.1016/j.ymsp.2015.08.033.
- [9] J. Li, S. He, J. R. R. A. Martins, M. Zhang, B. C. Khoo, Efficient data-driven off-design constraint modeling for practical aerodynamic shape optimization, *AIAA Journal* 61 (2023) 2854–2866. doi:10.2514/1.J062629.
- [10] P. Díaz-Morales, A. Corrochano, M. López-Martín, S. Le Clainche, Deep learning combined with singular value decomposition to reconstruct databases in fluid dynamics, *Expert Systems with Applications* 238 (2024) 121924. doi:10.1016/j.eswa.2023.121924.

- [11] K. SHIN, S. FERADAY, C. HARRIS, M. BRENNAN, J.-E. OH, Optimal autoregressive modelling of a measured noisy deterministic signal using singular-value decomposition, *Mechanical Systems and Signal Processing* 17 (2003) 423–432. doi:10.1006/mssp.2002.1510.
- [12] H. Pan, Y. Yang, J. Zheng, J. Cheng, A noise reduction method of symplectic singular mode decomposition based on lagrange multiplier, *Mechanical Systems and Signal Processing* 133 (2019) 106283. doi:10.1016/j.ymsp.2019.106283.
- [13] J. Li, Z. Chen, S. Li, Selection of the number of effective singular values for noise reduction, *Mechanical Systems and Signal Processing* 191 (2023) 110175. doi:10.1016/j.ymsp.2023.110175.
- [14] R. A. Sadek, Svd based image processing applications: State of the art, contributions and research challenges, *arXiv* (2012). doi:10.48550/ARXIV.1211.7102.
- [15] D. Wang, Adjustable robust singular value decomposition: Design, analysis and application to finance, *Data* 2 (2017) 29. doi:10.3390/data2030029.
- [16] S. d. Lucas, J. M. Vega, A. Velazquez, Aeronautic conceptual design optimization method based on high-order singular value decomposition, *AIAA Journal* 49 (2011) 2713–2725. doi:10.2514/1.j051133.
- [17] Y. Choi, G. Boncoraglio, S. Anderson, D. Amsallem, C. Farhat, Gradient-based constrained optimization using a database of linear reduced-order models, *Journal of Computational Physics* 423 (2020) 109787. doi:10.1016/j.jcp.2020.109787.
- [18] D. J. Poole, C. B. Allen, T. Rendall, Efficient aero-structural wing optimization using compact aerofoil decomposition, in: *AIAA Scitech 2019 Forum*, American Institute of Aeronautics and Astronautics, 2019. doi:10.2514/6.2019-1701.
- [19] J. Li, M. A. Bouhlel, J. R. R. A. Martins, A data-based approach for fast airfoil analysis and optimization, in: *2018 AIAA/ASCE/AHS/ASC Structures, Structural Dynamics, and Materials Conference*, Kissimmee, FL, 2018. doi:10.2514/6.2018-1383.

- [20] S. Li, J. Trevelyan, Z. Wu, H. Lian, D. Wang, W. Zhang, An adaptive svd–krylov reduced order model for surrogate based structural shape optimization through isogeometric boundary element method, *Computer Methods in Applied Mechanics and Engineering* 349 (2019) 312–338. doi:10.1016/j.cma.2019.02.023.
- [21] W. Yao, S. Marques, T. Robinson, C. Armstrong, L. Sun, A reduced-order model for gradient-based aerodynamic shape optimisation, *Aerospace Science and Technology* 106 (2020) 106120. doi:10.1016/j.ast.2020.106120.
- [22] J. Li, M. Zhang, Data-based approach for wing shape design optimization, *Aerospace Science and Technology* 112 (2021) 106639. doi:10.1016/j.ast.2021.106639.
- [23] N. Wu, C. A. Mader, J. R. R. A. Martins, Sensitivity-based geometric parametrization and automatic scaling for aerodynamic shape optimization, *AIAA Journal* 62 (2023) 231–246. doi:10.2514/1.J062661.
- [24] W. Chen, J. Kou, W. Yang, S. Pan, Dynamic-mode-decomposition-based gradient prediction for adjoint-based aerodynamic shape optimization, *Aerospace Science and Technology* 150 (2024) 109175. doi:10.1016/j.ast.2024.109175.
- [25] K. Liu, Application of svd in optimization of structural modal test, *Computers & structures* 63 (1997) 51–59. doi:10.1016/s0045-7949(96)00329-x.
- [26] T. H. Lee, An adjoint variable method for structural design sensitivity analysis of a distinct eigenvalue problem, *KSME International Journal* 13 (1999) 470–476. doi:10.1007/bf02947716.
- [27] H. Ersoy, A. Muğan, Design sensitivity analysis of structures based upon the singular value decomposition, *Computer Methods in Applied Mechanics and Engineering* 191 (2002) 3459–3476. doi:10.1016/s0045-7825(02)00259-1.
- [28] H. Ersoy, Optimum laminate design by using singular value decomposition, *Composites Part B: Engineering* 52 (2013) 144–154. doi:10.1016/j.compositesb.2013.04.005.

- [29] L. N. Trefethen, A. E. Trefethen, S. C. Reddy, T. A. Driscoll, Hydrodynamic stability without eigenvalues, *Science* 261 (1993) 578–584. doi:10.1126/science.261.5121.578.
- [30] P. J. Schmid, Dynamic mode decomposition of numerical and experimental data, *Journal of Fluid Mechanics* 656 (2010) 5–28. doi:10.1017/s0022112010001217.
- [31] K. Taira, M. S. Hemati, S. L. Brunton, Y. Sun, K. Duraisamy, S. Bagheri, S. T. M. Dawson, C.-A. Yeh, Modal analysis of fluid flows: Applications and outlook, *AIAA Journal* (2019) 1–25. doi:10.2514/1.j058462.
- [32] K. Taira, M. S. Hemati, S. L. Brunton, Y. Sun, K. Duraisamy, S. Bagheri, S. T. M. Dawson, C.-A. Yeh, Modal analysis of fluid flows: Applications and outlook, *AIAA Journal* 58 (2020) 998–1022. doi:10.2514/1.j058462.
- [33] G. H. Golub, C. F. Van Loan, *Matrix Computations*, 3rd ed., Johns Hopkins University Press, Baltimore, MD, 1996.
- [34] L. N. Trefethen, D. Bau III, *Numerical Linear Algebra*, SIAM: Society for Industrial and Applied Mathematics, 1997.
- [35] J. Demmel, K. Veselić, Jacobi’s method is more accurate than qr, *SIAM Journal on Matrix Analysis and Applications* 13 (1992) 1204–1245. doi:10.1137/0613074.
- [36] Y. Saad, *Numerical Methods for Large Eigenvalue Problems: Revised Edition*, Society for Industrial and Applied Mathematics, 2011. doi:10.1137/1.9781611970739.
- [37] N. Halko, P. G. Martinsson, J. A. Tropp, Finding structure with randomness: Probabilistic algorithms for constructing approximate matrix decompositions, *SIAM Review* 53 (2011) 217–288. doi:10.1137/090771806.
- [38] Z. Zhang, *The singular value decomposition, applications and beyond*, 2015. doi:10.48550/ARXIV.1510.08532.

- [39] A. J. Salgado, S. M. Wise, *Classical Numerical Analysis: A Comprehensive Course*, Cambridge University Press, 2022. doi:10.1017/9781108942607.
- [40] H. Schwerdtfeger, *Introduction to linear algebra and the theory of matrices*, 1961.
- [41] O. Makkonen, C. Hollanti, Secure distributed gram matrix multiplication, in: *2023 IEEE Information Theory Workshop (ITW)*, IEEE, 2023. doi:10.1109/itw55543.2023.10161614.
- [42] S. He, Y. Shi, E. Jonsson, J. R. R. A. Martins, Eigenvalue problem derivatives computation for a complex matrix using the adjoint method, *Mechanical Systems and Signal Processing* 185 (2023) 109717. doi:10.1016/j.ymssp.2022.109717.
- [43] S. Ragnarsson, C. F. Van Loan, Block tensors and symmetric embeddings, *Linear Algebra and its Applications* 438 (2013) 853–874. doi:10.1016/j.laa.2011.04.014.
- [44] P. C. Hansen, *Rank-Deficient and Discrete Ill-Posed Problems: Numerical Aspects of Linear Inversion*, Society for Industrial and Applied Mathematics, 1998. doi:10.1137/1.9780898719697.
- [45] G. W. Stewart, *Perturbation theory for the singular value decomposition*, Citeseer, 1998.
- [46] V. Angelova, P. Petkov, Componentwise perturbation analysis of the singular value decomposition of a matrix, *Applied Sciences* 14 (2024) 1417. doi:10.3390/app14041417.
- [47] P. I. Davies, M. I. Smith, Updating the singular value decomposition, *Journal of Computational and Applied Mathematics* 170 (2004) 145–167. doi:10.1016/j.cam.2003.12.039.
- [48] R. M. Lin, J. E. Mottershead, T. Y. Ng, A state-of-the-art review on theory and engineering applications of eigenvalue and eigenvector derivatives, *Mechanical Systems and Signal Processing* 138 (2020) 106536. doi:10.1016/j.ymssp.2019.106536.

- [49] X. García Santiago, Numerical methods for shape optimization of photonic nanostructures (2021). doi:10.5445/IR/1000131006.
- [50] C. S. Skene, P. J. Schmid, Adjoint-based parametric sensitivity analysis for swirling m-flames, *Journal of Fluid Mechanics* 859 (2018) 516–542. doi:10.1017/jfm.2018.793.
- [51] J. R. R. A. Martins, A. Ning, *Engineering Design Optimization*, Cambridge University Press, Cambridge, UK, 2022. URL: <https://mdobook.github.io>. doi:10.1017/9781108980647.
- [52] J. R. R. A. Martins, J. T. Hwang, Review and unification of methods for computing derivatives of multidisciplinary computational models, *AIAA Journal* 51 (2013) 2582–2599. doi:10.2514/1.J052184.
- [53] J. R. R. A. Martins, P. Sturdza, J. J. Alonso, The complex-step derivative approximation, *ACM Transactions on Mathematical Software* 29 (2003) 245–262. doi:10.1145/838250.838251.
- [54] Z. Lyu, Z. Xu, J. R. R. A. Martins, Benchmarking optimization algorithms for wing aerodynamic design optimization, in: *Proceedings of the 8th International Conference on Computational Fluid Dynamics*, Chengdu, Sichuan, China, 2014. ICCFD8-2014-0203.
- [55] M. B. Giles, N. A. Pierce, An introduction to the adjoint approach to design, *Flow, Turbulence and Combustion* 65 (2000) 393–415. doi:10.1023/A:1011430410075.
- [56] J. Townsend, Differentiating the singular value decomposition, Technical Report, Technical Report 2016, 2016.
- [57] M. Seeger, A. Hetzel, Z. Dai, E. Meissner, N. D. Lawrence, Auto-differentiating linear algebra, *arXiv* (2017). doi:10.48550/ARXIV.1710.08717.
- [58] Z.-Q. Wan, S.-X. Zhang, Automatic differentiation for complex valued svd, 2019. doi:10.48550/ARXIV.1909.02659.
- [59] S. He, E. Jonsson, J. R. R. A. Martins, Derivatives for eigenvalues and eigenvectors via analytic reverse algorithmic differentiation, *AIAA Journal* 60 (2022) 2654–2667. doi:10.2514/1.J060726.

- [60] L. Jin, T. A. Zaki, From streaks to spots and on to turbulence: exploring the dynamics of boundary layer transition, *Flow, Turbulence and Combustion* 91 (2013) 451–473. doi:10.7281/T17S7KX8.
- [61] M. B. Giles, *Collected matrix derivative results for forward and reverse mode algorithmic differentiation*, Springer, 2008, pp. 35–44. doi:10.1007/978-3-540-68942-3_4.
- [62] J. Bradbury, R. Frostig, P. Hawkins, M. J. Johnson, C. Leary, D. Maclaurin, G. Necula, A. Paszke, J. VanderPlas, S. Wanderman-Milne, Q. Zhang, *JAX: composable transformations of Python+NumPy programs*, 2018.
- [63] C. R. Harris, K. J. Millman, S. J. van der Walt, R. Gommers, P. Virtanen, D. Cournapeau, E. Wieser, J. Taylor, S. Berg, N. J. Smith, R. Kern, M. Picus, S. Hoyer, M. H. van Kerkwijk, M. Brett, A. Haldane, J. del Río, M. Wiebe, P. Peterson, P. Gérard-Marchant, K. Sheppard, T. Reddy, W. Weckesser, H. Abbasi, C. Gohlke, T. E. Oliphant, *Array programming with NumPy*, *Nature* 585 (2020) 357–362. doi:10.1038/s41586-020-2649-2.
- [64] J. Hunt, Vorticity and vortex dynamics in complex turbulent flows, *Transactions of the Canadian Society for Mechanical Engineering* 11 (1987) 21–35. doi:10.1139/tcsme-1987-0004.
- [65] D. A. Roberts, L. R. Roberts, Qr and lq decomposition matrix backpropagation algorithms for square, wide, and deep–real or complex–matrices and their software implementation, *arXiv preprint arXiv:2009.10071* (2020). doi:10.48550/ARXIV.2009.10071.
- [66] M. Giles, *An extended collection of matrix derivative results for forward and reverse mode algorithmic differentiation*, 2008.
- [67] A. Hjørungnes, *Complex-Valued Matrix Derivatives: With Applications in Signal Processing and Communications*, Cambridge University Press, 2011. doi:10.1017/cbo9780511921490.
- [68] A. Hjørungnes, D. Gesbert, Complex-valued matrix differentiation: Techniques and key results, *IEEE Transactions on Signal Processing* 55 (2007) 2740–2746. doi:10.1109/tsp.2007.893762.

Appendix A. Adjoint method for EVP

We derive the adjoint equation for any function, $f = f(\mathbf{w}, \mathbf{D}(\mathbf{x}))$, where \mathbf{D} is the input EVP coefficient matrix and \mathbf{w} is the solution of the EVP. The coefficient matrix can be further parametrized by design variable, \mathbf{x} . Thus, expanding the adjoint equations Eq. (13) and Eq. (14) from Section 2, we have

$$\begin{bmatrix} \mathbf{D}_r - \lambda_r \mathbf{I} & -\mathbf{D}_i + \lambda_i \mathbf{I} & -\phi_r & \phi_i \\ \mathbf{D}_i - \lambda_i \mathbf{I} & \mathbf{D}_r + \lambda_r \mathbf{I} & -\phi_i & -\phi_r \\ 2\phi_r^\top & 2\phi_i^\top & 0 & 0 \\ 0 & \mathbf{e}_k^\top & 0 & 0 \end{bmatrix} \begin{bmatrix} \psi_{\text{main},r} \\ \psi_{\text{main},i} \\ \psi_m \\ \psi_p \end{bmatrix} = \frac{\partial f^\top}{\partial \mathbf{w}}, \quad (\text{A.1})$$

which is the adjoint equation for the EVP of matrix \mathbf{D} . The partial derivative of the residual matrix with respect to the complex parts of the matrix \mathbf{D} is

$$\begin{aligned} \frac{\partial \mathbf{r}}{\partial \mathbf{D}_r} &= \psi_{\text{main},r} \phi_r^\top + \psi_{\text{main},i} \phi_i^\top, \\ \frac{\partial \mathbf{r}}{\partial \mathbf{D}_i} &= -\psi_{\text{main},r} \phi_i^\top + \psi_{\text{main},i} \phi_r^\top, \end{aligned} \quad (\text{A.2})$$

and the partial derivatives of complex components of f with respect to those of the matrix \mathbf{D} are

$$\begin{aligned} \frac{df_r}{d\mathbf{D}_r} &= -\frac{\partial \mathbf{r}^\top}{\partial \mathbf{D}_r} \psi_r, \\ \frac{df_r}{d\mathbf{D}_i} &= -\frac{\partial \mathbf{r}^\top}{\partial \mathbf{D}_i} \psi_r, \\ \frac{df_i}{d\mathbf{D}_r} &= -\frac{\partial \mathbf{r}^\top}{\partial \mathbf{D}_r} \psi_i, \\ \frac{df_i}{d\mathbf{D}_i} &= -\frac{\partial \mathbf{r}^\top}{\partial \mathbf{D}_i} \psi_i. \end{aligned} \quad (\text{A.3})$$

This completes the adjoint method for solving EVP. Detailed approach can be found in He et al [42].

Appendix B. Chain rule RAD formula

Consider the matrix $\mathbf{B} = \mathbf{A}\mathbf{A}^*$. An FAD application on both sides results in the real part as

$$\dot{\mathbf{B}}_r = \dot{\mathbf{A}}_r \mathbf{A}_r^\top + \mathbf{A}_r \dot{\mathbf{A}}_r^\top + \dot{\mathbf{A}}_i \mathbf{A}_i^\top + \mathbf{A}_i \dot{\mathbf{A}}_i^\top, \quad (\text{B.1})$$

and the imaginary part as

$$\dot{\mathbf{B}}_i = \dot{\mathbf{A}}_i \mathbf{A}_r^\top + \mathbf{A}_i \dot{\mathbf{A}}_r^\top - \dot{\mathbf{A}}_r \mathbf{A}_i^\top - \mathbf{A}_r \dot{\mathbf{A}}_i^\top. \quad (\text{B.2})$$

These two terms $\dot{\mathbf{B}}_r$ and $\dot{\mathbf{B}}_i$ can be used in the Trace expression in Eq. (J.4) as

$$\text{Tr}[\overline{\mathbf{B}}_r^\top \dot{\mathbf{B}}_r + \overline{\mathbf{B}}_i^\top \dot{\mathbf{B}}_i] = \text{Tr}[\overline{\mathbf{A}}_r^\top \dot{\mathbf{A}}_r + \overline{\mathbf{A}}_i^\top \dot{\mathbf{A}}_i]. \quad (\text{B.3})$$

Upon applying the Tr identities and expanding LHS of Eq. (B.3), we have

$$\begin{aligned} \text{Tr}[(\mathbf{A}_r^\top \overline{\mathbf{B}}_r^\top + \mathbf{A}_r^\top \overline{\mathbf{B}}_r + \mathbf{A}_i^\top \overline{\mathbf{B}}_i - \mathbf{A}_i^\top \overline{\mathbf{B}}_i^\top) \dot{\mathbf{A}}_r + \\ (\mathbf{A}_i^\top \overline{\mathbf{B}}_r^\top + \mathbf{A}_i^\top \overline{\mathbf{B}}_r + \mathbf{A}_r^\top \overline{\mathbf{B}}_i^\top - \mathbf{A}_r^\top \overline{\mathbf{B}}_i) \dot{\mathbf{A}}_i] \\ = \text{Tr}[\overline{\mathbf{A}}_r^\top \dot{\mathbf{A}}_r + \overline{\mathbf{A}}_i^\top \dot{\mathbf{A}}_i], \end{aligned} \quad (\text{B.4})$$

which upon simplifying we get for the real part

$$\overline{\mathbf{A}}_r = (\mathbf{A}_r^\top \overline{\mathbf{B}}_r^\top + \mathbf{A}_r^\top \overline{\mathbf{B}}_r + \mathbf{A}_i^\top \overline{\mathbf{B}}_i - \mathbf{A}_i^\top \overline{\mathbf{B}}_i^\top)^\top, \quad (\text{B.5})$$

and for the imaginary part

$$\overline{\mathbf{A}}_i = (\mathbf{A}_i^\top \overline{\mathbf{B}}_r^\top + \mathbf{A}_i^\top \overline{\mathbf{B}}_r + \mathbf{A}_r^\top \overline{\mathbf{B}}_i^\top - \mathbf{A}_r^\top \overline{\mathbf{B}}_i)^\top. \quad (\text{B.6})$$

Now we can place the reverse seed as g_r and g_i in each of the Eq. (B.5) and Eq. (B.6) to obtain the derivatives as in Eq. (20).

Consider then the matrix $\mathbf{C} = \mathbf{A}^* \mathbf{A}$ Following the same methods as in Eqs. (B.3) to (B.6), we have for the real part

$$\overline{\mathbf{A}}_r = (\overline{\mathbf{C}}_r \mathbf{A}_r^\top + \overline{\mathbf{C}}_r^\top \mathbf{A}_r^\top + \overline{\mathbf{C}}_i \mathbf{A}_i^\top - \overline{\mathbf{C}}_i^\top \mathbf{A}_i^\top)^\top, \quad (\text{B.7})$$

and for the imaginary part

$$\overline{\mathbf{A}}_i = (\overline{\mathbf{C}}_r \mathbf{A}_i^\top + \overline{\mathbf{C}}_r^\top \mathbf{A}_i^\top + \overline{\mathbf{C}}_i \mathbf{A}_r^\top - \overline{\mathbf{C}}_i^\top \mathbf{A}_r^\top)^\top. \quad (\text{B.8})$$

We can then seed h_r and h_i each into Eqs. (B.7) and (B.8) to obtain the derivatives in Eq. (25).

Appendix C. Vectorization

The vectorization operator $\text{vec}(\cdot)$ is defined as

$$(\text{vec}(\mathbf{A}))_{i \times (n_2 - 1) + j} = \mathbf{A}_{ij}, \quad i = 1, \dots, n_1, \quad j = 1, \dots, n_2, \quad (\text{C.1})$$

where $\mathbf{A} \in \mathbb{R}^{n_1 \times n_2}$, $\text{vec} : \mathbb{R}^{n_1 \times n_2} \rightarrow \mathbb{R}^{n_1 n_2}$, and the subscript represents the index of an element from the matrix \mathbf{A} or the vector $\text{vec}(\mathbf{A})$. This linear operation transforms a matrix into a vector simplifying the matrix derivative computation. The inverse vectorization operator $\text{vec}^{-1}(\cdot)$ is defined as,

$$\text{vec}^{-1}(\text{vec}(\mathbf{A})) = \mathbf{A}, \quad (\text{C.2})$$

for arbitrary matrix \mathbf{A} . As a special case of the properties of vectorization,

$$\begin{aligned} \text{vec}(\mathbf{a}) &= \mathbf{a}, \\ \text{vec}^{-1}(\mathbf{a}) &= \mathbf{a}, \end{aligned} \quad (\text{C.3})$$

where $\mathbf{a} \in \mathbb{R}^{n_3}$ is some arbitrary vector.

The following convention is used when writing a derivative involving matrices in this paper for $(\partial \mathbf{A} / \partial \mathbf{B})^\top \bar{\mathbf{A}}$, where $\mathbf{A} \in \mathbb{R}^{n_1 \times n_2}$, and $\mathbf{B} \in \mathbb{R}^{n_2 \times n_3}$. Using the vectorization notation, $(\partial \mathbf{A} / \partial \mathbf{B})^\top \bar{\mathbf{A}}$ is a simplified notation of

$$\text{vec}^{-1} \left(\left(\frac{\partial \text{vec}(\mathbf{A})}{\partial \text{vec}(\mathbf{B})} \right)^\top \text{vec}(\bar{\mathbf{A}}) \right) \in \mathbb{R}^{n_2 \times n_3}. \quad (\text{C.4})$$

This signifies the computation of the tensor-vector products such as seen in Eqs. (20) and (25).

Appendix D. RAD form for GMM

Consider the governing equation for SVD as shown in Eq. (8). The vector \mathbf{u} can be written as

$$\mathbf{u} = \frac{\mathbf{A}\mathbf{v}}{\sigma}, \quad (\text{D.1})$$

which can be re-written in terms of the real and imaginary parts as

$$\begin{aligned} \mathbf{u}_r &= \mathbf{A}_r \mathbf{v}_r \frac{1}{\sigma} - \mathbf{A}_i \mathbf{v}_i \frac{1}{\sigma}, \\ \mathbf{u}_i &= \mathbf{A}_r \mathbf{v}_i \frac{1}{\sigma} - \mathbf{A}_i \mathbf{v}_r \frac{1}{\sigma}. \end{aligned} \quad (\text{D.2})$$

Applying the dot product identity from Appendix J and considering the contribution from \mathbf{A} , we have

$$\begin{aligned}\bar{\mathbf{A}}_r &= \frac{1}{\sigma} \left(\bar{\mathbf{u}}_r \mathbf{v}_r^\top + \bar{\mathbf{u}}_i \mathbf{v}_i^\top \right), \\ \bar{\mathbf{A}}_i &= \frac{1}{\sigma} \left(\bar{\mathbf{u}}_i \mathbf{v}_r^\top - \bar{\mathbf{u}}_r \mathbf{v}_i^\top \right).\end{aligned}\tag{D.3}$$

Consider then the same governing equation for SVD as described in Eq. (8). For the second route taken for the Adjoint-based derivative computation described in Section 3.2, the vector \mathbf{v} is expressed in terms of the remaining singular variables as

$$\mathbf{v} = \frac{\mathbf{A}^* \mathbf{u}}{\sigma}.\tag{D.4}$$

Thus, through trace identities from Appendix J, we have

$$\begin{aligned}\bar{\mathbf{A}}_r &= \frac{1}{\sigma} \left(\mathbf{u}_r \bar{\mathbf{v}}_r^\top + \mathbf{u}_i \bar{\mathbf{v}}_i^\top \right), \\ \bar{\mathbf{A}}_i &= \frac{1}{\sigma} \left(\mathbf{u}_i \bar{\mathbf{v}}_r^\top - \mathbf{u}_r \bar{\mathbf{v}}_i^\top \right).\end{aligned}\tag{D.5}$$

This concludes the derivation of for the term in the brackets of Eqs. (20) and (25).

Appendix E. Derivation of Eq. (29)

Consider the residual form $\mathbf{r}(\mathbf{w})$ in Eq. (9). Upon differentiating this with respect to \mathbf{A}_r , we have in FAD notation

$$\dot{\mathbf{r}} = \begin{bmatrix} \dot{\mathbf{A}}_r \mathbf{v}_r \\ \dot{\mathbf{A}}_r \mathbf{v}_i \\ \dot{\mathbf{A}}_r^\top \mathbf{u}_r \\ \dot{\mathbf{A}}_r^\top \mathbf{u}_i \\ 0 \\ 0 \end{bmatrix}.\tag{E.1}$$

Applying the dot product identity for real valued functions here, we have

$$\text{Tr}(\bar{\mathbf{r}}^\top \dot{\mathbf{r}}) = \text{Tr}(\bar{\mathbf{A}}_r^\top \dot{\mathbf{A}}_r).\tag{E.2}$$

Placing the adjoint vector $\boldsymbol{\psi}$ as a reverse seed here, we get

$$\text{Tr}(\bar{\mathbf{r}}^\top \dot{\mathbf{r}}) = \text{Tr}(\boldsymbol{\psi}^\top \dot{\mathbf{r}}), \quad (\text{E.3})$$

which upon expanding the RHS, we get the expression

$$\text{Tr}(\boldsymbol{\psi}_{v_r}^\top \dot{\mathbf{A}}_r \mathbf{v}_r + \boldsymbol{\psi}_{v_i}^\top \dot{\mathbf{A}}_r \mathbf{v}_i + \boldsymbol{\psi}_{u_r}^\top \dot{\mathbf{A}}_r^\top \mathbf{u}_r + \boldsymbol{\psi}_{u_i}^\top \dot{\mathbf{A}}_r^\top \mathbf{u}_i), \quad (\text{E.4})$$

and then applying the trace identities and re-arranging terms, we get

$$\text{Tr}((\mathbf{v}_r \boldsymbol{\psi}_{v_r}^\top + \mathbf{v}_i \boldsymbol{\psi}_{v_i}^\top + \boldsymbol{\psi}_{u_r} \mathbf{u}_r^\top + \boldsymbol{\psi}_{u_i} \mathbf{u}_i^\top) \dot{\mathbf{A}}_r) = \text{Tr}(\bar{\mathbf{A}}_r^\top \dot{\mathbf{A}}_r). \quad (\text{E.5})$$

Since this must hold for any arbitrary $\dot{\mathbf{A}}_r$, we have

$$\bar{\mathbf{A}}_r = \boldsymbol{\psi}_{v_r} \mathbf{v}_r^\top + \boldsymbol{\psi}_{v_i} \mathbf{v}_i^\top + \mathbf{u}_r \boldsymbol{\psi}_{u_r}^\top + \mathbf{u}_i \boldsymbol{\psi}_{u_i}^\top. \quad (\text{E.6})$$

Similarly taking the derivative of $\mathbf{r}(\mathbf{w})$ in Eq. (9) with respect to \mathbf{A}_i and following a similar procedure as described above, we have

$$\bar{\mathbf{A}}_i = -\boldsymbol{\psi}_{v_r} \mathbf{v}_i^\top + \boldsymbol{\psi}_{v_i} \mathbf{v}_r^\top + \mathbf{u}_i \boldsymbol{\psi}_{u_r}^\top - \mathbf{u}_r \boldsymbol{\psi}_{u_i}^\top. \quad (\text{E.7})$$

This concludes our derivation of Eq. (29). It must be noted that the derivative here is $(\partial \mathbf{r} / \partial \mathbf{A})^\top \boldsymbol{\psi}$. It is obtained by reverse seeding the residual vector \mathbf{r} .

Appendix F. Singular value derivative using RAD

Consider the singular value (dominant) written in terms of the complex matrix, \mathbf{A} , and its corresponding singular vectors as

$$\sigma = \mathbf{u}^* \mathbf{A} \mathbf{v}, \quad (\text{F.1})$$

where “ \square^* ” represents the complex conjugate operation. \mathbf{u} and \mathbf{v} are the left and right singular vectors respectively for the singular value. We will now derive the derivative of this singular value with respect to the matrix \mathbf{A} . Eq. (F.1) can be re-written as

$$\begin{aligned}
\mathbf{A}\mathbf{v} &= \sigma\mathbf{u}, \\
\Rightarrow \dot{\mathbf{A}}\mathbf{v} + \mathbf{A}\dot{\mathbf{v}} &= \dot{\sigma}\mathbf{u} + \sigma\dot{\mathbf{u}}, \\
\Rightarrow \mathbf{u}^*\dot{\mathbf{A}}\mathbf{v} + \mathbf{u}^*\mathbf{A}\dot{\mathbf{v}} &= \mathbf{u}^*\dot{\sigma}\mathbf{u} + \sigma\mathbf{u}^*\dot{\mathbf{u}}, \\
\Rightarrow \mathbf{u}^*\dot{\mathbf{A}}\mathbf{v} + \mathbf{u}^*\mathbf{U}\Sigma\mathbf{V}^*\dot{\mathbf{v}} &= \mathbf{u}^*\dot{\sigma}\mathbf{u} + \sigma\mathbf{u}^*\dot{\mathbf{u}}, \\
\Rightarrow \mathbf{u}^*\dot{\mathbf{A}}\mathbf{v} + \sigma\mathbf{v}^*\dot{\mathbf{v}} &= \mathbf{u}^*\dot{\sigma}\mathbf{u} + \sigma\mathbf{u}^*\dot{\mathbf{u}}, \\
\Rightarrow \mathbf{u}^*\dot{\mathbf{A}}\mathbf{v} &= \dot{\sigma},
\end{aligned} \tag{F.2}$$

where going from the second from last to the last equation, we used the fact that $\mathbf{u}^*\mathbf{u} = \mathbf{v}^*\mathbf{v} = 1$, thus, $\dot{\mathbf{u}}^*\mathbf{u} = \dot{\mathbf{v}}^*\mathbf{v} = 0$.

Expanding the final equation in Eq. (F.2) into its real and imaginary parts, we have

$$\begin{aligned}
\dot{\sigma} &= \mathbf{u}_r^T \dot{\mathbf{A}}_r \mathbf{v}_r + \mathbf{u}_i^T \dot{\mathbf{A}}_i \mathbf{v}_r - \mathbf{u}_r^T \dot{\mathbf{A}}_i \mathbf{v}_i + \mathbf{u}_i^T \dot{\mathbf{A}}_r \mathbf{v}_i \\
&\quad + i(\mathbf{u}_r^T \dot{\mathbf{A}}_i \mathbf{v}_r - \mathbf{u}_i^T \dot{\mathbf{A}}_r \mathbf{v}_r + \mathbf{u}_r^T \dot{\mathbf{A}}_r \mathbf{v}_i + \mathbf{u}_i^T \dot{\mathbf{A}}_i \mathbf{v}_i),
\end{aligned} \tag{F.3}$$

where the imaginary part is zero because the singular value is a real number. Thus,

$$\dot{\sigma} = \mathbf{u}_r^T \dot{\mathbf{A}}_r \mathbf{v}_r + \mathbf{u}_i^T \dot{\mathbf{A}}_i \mathbf{v}_r - \mathbf{u}_r^T \dot{\mathbf{A}}_i \mathbf{v}_i + \mathbf{u}_i^T \dot{\mathbf{A}}_r \mathbf{v}_i, \tag{F.4}$$

which is the final FAD form to begin with for applying the dot product identity formula from Giles [61] as

$$\text{Tr}(\bar{\sigma}^T \dot{\sigma}) = \text{Tr}\left(\bar{\sigma}^T(\mathbf{u}_r^T \dot{\mathbf{A}}_r \mathbf{v}_r + \mathbf{u}_i^T \dot{\mathbf{A}}_i \mathbf{v}_r - \mathbf{u}_r^T \dot{\mathbf{A}}_i \mathbf{v}_i + \mathbf{u}_i^T \dot{\mathbf{A}}_r \mathbf{v}_i)\right), \tag{F.5}$$

Applying trace identities, we can re write it for \mathbf{A}_r as

$$\text{Tr}\left(\bar{\sigma}^T(\mathbf{v}_r \mathbf{u}_r^T + \mathbf{v}_i \mathbf{u}_i^T) \dot{\mathbf{A}}_r\right) = \text{Tr}\left(\bar{\mathbf{A}}_r^T \dot{\mathbf{A}}_r\right). \tag{F.6}$$

This has to hold for any arbitrary $\dot{\mathbf{A}}_r$. Thus, we have

$$\bar{\mathbf{A}}_r = (\mathbf{u}_r \mathbf{v}_r^T + \mathbf{u}_i \mathbf{v}_i^T) \bar{\sigma}. \tag{F.7}$$

Similarly for \mathbf{A}_i , we have:

$$\text{Tr}\left(\bar{\sigma}^T(\mathbf{v}_r \mathbf{u}_i^T - \mathbf{v}_i \mathbf{u}_r^T) \dot{\mathbf{A}}_r\right) = \text{Tr}\left(\bar{\mathbf{A}}_i^T \dot{\mathbf{A}}_i\right). \tag{F.8}$$

This has to hold for any arbitrary $\dot{\mathbf{A}}_i$. Thus, we have

$$\bar{\mathbf{A}}_i = (-\mathbf{u}_r \mathbf{v}_i^\top + \mathbf{u}_i \mathbf{v}_r^\top) \bar{\sigma}. \quad (\text{F.9})$$

Placing the reverse seed of $\bar{\sigma}$ equal to 1 in Eq. (F.7) and Eq. (F.9), we can obtain the partial derivatives $d\sigma_r/d\mathbf{A}_r$ and $d\sigma_r/d\mathbf{A}_i$.

In the real dimension, we will have upon placing the reverse seed of $\bar{\sigma}$ equal to 1 in Eq. (F.7),

$$\frac{d\sigma}{d\mathbf{A}} = \mathbf{u}\mathbf{v}^\top, \quad (\text{F.10})$$

where $\mathbf{u} \in \mathbb{R}$ and $\mathbf{v} \in \mathbb{R}$. This concludes the derivation for Eq. (30).

Appendix G. Adjoint method Jacobian computation and direct contribution of main matrix

Consider the objective function f as

$$f = \mathbf{c}^\top \mathbf{u}, \quad (\text{G.1})$$

where \mathbf{c} is a complex constant vector and \mathbf{u} is the left singular vector. The function f can be written in its real and imaginary parts as $f = f_r + if_i$. The real and imaginary parts are

$$\begin{aligned} f_r &= \mathbf{c}_r^\top \mathbf{u}_r - \mathbf{c}_i^\top \mathbf{u}_i, \\ f_i &= \mathbf{c}_r^\top \mathbf{u}_i + \mathbf{c}_i^\top \mathbf{u}_r. \end{aligned} \quad (\text{G.2})$$

Here, the Jacobian of the components of f (f_r and f_i) with respect to the state variables \mathbf{w} for the SEMM case is $\partial f/\partial \mathbf{w}$ where \mathbf{w} can be taken from Eq. (9). The Jacobian for f_r will then look like

$$\frac{\partial f_r}{\partial \mathbf{w}} = \begin{bmatrix} \mathbf{c}_r \\ -\mathbf{c}_i \\ 0 \\ 0 \\ 0 \\ 0 \end{bmatrix}. \quad (\text{G.3})$$

Similarly the Jacobian for f_i will look like

$$\frac{\partial f_i}{\partial \mathbf{w}} = \begin{bmatrix} \mathbf{c}_i \\ \mathbf{c}_r \\ 0 \\ 0 \\ 0 \\ 0 \end{bmatrix}. \quad (\text{G.4})$$

Once we have these Jacobians, we can proceed with the derivative computation method discussed in Section 4, particularly from Eq. (27) since we now have its RHS. A similar approach can be shown for the Eqs. (16) and (21) in the GMM case for formation of the Jacobian and hence the RHS of the adjoint equations. It can be seen however that this is simply cumbersome even for such a simple linear function as shown in Eq. (G.1).

Thus, JAX [62] was used for this step, and so can any other equivalent automatic differentiation tool be used to save implementation effort and time. The same approach can be taken for the direct dependencies of the function on the matrix \mathbf{A} , if any. If the dependency arises from the GMM computation, then the formulae shown in Appendix D can be used, as pointed out in Section 3.2. These formulae are based on the automatic differentiation and hence are equivalent when either this approach or the JAX approach is used for evaluation of this step.

Appendix H. FD formula

A finite difference formula (FD) was employed to compare the results from the proposed Adjoint and RAD methods for the singular value derivative in Section 4.1 and Section 4.2. The following equations were employed for the

FD results in Tables 2 to 5.

$$\begin{aligned}
\frac{df_r}{d\mathbf{A}_{r,pq}} &= \operatorname{Re} \left(\frac{f(\mathbf{A} + \epsilon \mathbf{E}_{pq}) - f(\mathbf{A})}{\epsilon} \right), \\
\frac{df_r}{d\mathbf{A}_{i,pq}} &= \operatorname{Im} \left(\frac{f(\mathbf{A} + i\epsilon \mathbf{E}_{pq}) - f(\mathbf{A})}{\epsilon} \right), \\
\frac{df_i}{d\mathbf{A}_{r,pq}} &= \operatorname{Re} \left(\frac{f(\mathbf{A} + \epsilon \mathbf{E}_{pq}) - f(\mathbf{A})}{\epsilon} \right), \\
\frac{df_i}{d\mathbf{A}_{i,pq}} &= \operatorname{Im} \left(\frac{f(\mathbf{A} + i\epsilon \mathbf{E}_{pq}) - f(\mathbf{A})}{\epsilon} \right),
\end{aligned} \tag{H.1}$$

where $\epsilon = 10^{-6}$ is the finite perturbation applied to the matrix \mathbf{A} , \mathbf{E}_{pq} is a single entry matrix with the element on p^{th} row and q^{th} column set equal to ϵ and the remaining elements set to zero.

Appendix I. The method of snapshots

In the method of snapshots, a covariance matrix is formed using the equation

$$\mathbf{C} = \mathbf{X}^T \mathbf{X}, \tag{I.1}$$

where \mathbf{X} is the snapshot data matrix. The EVP of \mathbf{X} is then solved to get the eigenvectors and eigenvalues

$$\mathbf{C} \mathbf{v}_i = \lambda_i \mathbf{v}_i. \tag{I.2}$$

The POD modes are then simply

$$\Phi_i = \mathbf{X} \mathbf{v}_i \frac{1}{\sqrt{\lambda_i}}, \tag{I.3}$$

where i denotes each mode level. The energy levels are related to λ , and the singular values from the SVD are simply the square roots of all the λ_i .

The eigenvectors \mathbf{v}_i are the same as the right singular vectors of SVD of \mathbf{X} and are related to the temporal coefficients. The temporal coefficients can be calculated as

$$a_i(t) = \mathbf{v}_i \sqrt{\lambda_i}, \tag{I.4}$$

where t is the physical time step value.

Appendix J. RAD dot product identities and chain rule

We propose the dot product identity for complex differentiable function (in multivariate sense). For real valued matrices, $\mathbf{A} \in \mathbb{R}^{m_1 \times n_1}$, and functions of those matrices, $\mathbf{B}(\mathbf{A}) : \mathbb{R}^{m_1 \times n_1} \rightarrow \mathbb{R}^{m_2 \times n_2}$, Giles [61] proposed the following dot product identity

$$\text{Tr} \left(\overline{\mathbf{B}}^\top \dot{\mathbf{B}} \right) = \text{Tr} \left((\overline{\mathbf{A}}^\top \dot{\mathbf{A}}) \right), \quad (\text{J.1})$$

where \mathbf{B} is a real differentiable function of \mathbf{A} .

He et al [42] proposed the following identity for complex matrices, $\mathbf{A} \in \mathbb{C}^{m_1 \times n_1}$, and analytic matrix functions of those matrices, $\mathbf{B}(\mathbf{A}) : \mathbb{C}^{m_1 \times n_1} \rightarrow \mathbb{C}^{m_2 \times n_2}$

$$\text{Tr} \left(\overline{\mathbf{B}}^* \dot{\mathbf{B}} \right) = \text{Tr} \left(\overline{\mathbf{A}}^* \dot{\mathbf{A}} \right), \quad (\text{J.2})$$

where the tranpose operator, \square^\top , is replaced by the conjugate transpose operator, \square^* .

However, for complex differentiable function (in multivariate sense) but not complex non-analytic functions, the conjugate variables need to be considered. After applying the Wirtinger derivatives, Roberts and Roberts proposed the following RAD trace-identity for complex matrices and their non-analytic functions:

$$\text{Tr} \left(\overline{\mathbf{B}}^* \dot{\mathbf{B}} + (\overline{\mathbf{B}}^* \dot{\mathbf{B}})^* \right) = \text{Tr} \left(\overline{\mathbf{A}}^* \dot{\mathbf{A}} + (\overline{\mathbf{A}}^* \dot{\mathbf{A}})^* \right). \quad (\text{J.3})$$

Notice that for \mathbf{B} being an analytic function of \mathbf{A} , the second term in the Trace operator on each side of Eq. (J.3) becomes zero, effectively reducing to Eq. (J.2).

We can also expand Eq. (J.3) into real and imaginary components which is more convinient to deal with in many cases where the real and imaginary components are derived separately. Eq. (J.3) can be written as

$$\text{Tr} \left(\overline{\mathbf{B}}_r^\top \dot{\mathbf{B}}_r + \overline{\mathbf{B}}_i^\top \dot{\mathbf{B}}_i \right) = \text{Tr} \left(\overline{\mathbf{A}}_r^\top \dot{\mathbf{A}}_r + \overline{\mathbf{A}}_i^\top \dot{\mathbf{A}}_i \right), \quad (\text{J.4})$$

where we used the trace identity that $\text{Tr}(\mathbf{A}) = \text{Tr}(\mathbf{A}^\top)$.

Table J.6: RAD trace identity for different matrix functions.

	Formula
Real differentiable	$\text{Tr}(\overline{\mathbf{B}}^T \dot{\mathbf{B}}) = \text{Tr}(\overline{\mathbf{A}}^T \dot{\mathbf{A}})$ (Giles [61])
Complex analytic	$\text{Tr}(\overline{\mathbf{B}}^* \dot{\mathbf{B}}) = \text{Tr}(\overline{\mathbf{A}}^* \dot{\mathbf{A}})$ (He et al. [42])
	$\text{Tr}(\overline{\mathbf{B}}^* \dot{\mathbf{B}} + (\overline{\mathbf{B}}^* \dot{\mathbf{B}})^*) = \text{Tr}(\overline{\mathbf{A}}^* \dot{\mathbf{A}} + (\overline{\mathbf{A}}^* \dot{\mathbf{A}})^*)$ (Roberts and Roberts [65])
Complex multivariate differentiable	$\text{Tr}(\overline{\mathbf{B}}_r^T \dot{\mathbf{B}}_r + \overline{\mathbf{B}}_i^T \dot{\mathbf{B}}_i) = \text{Tr}(\overline{\mathbf{A}}_r^T \dot{\mathbf{A}}_r + \overline{\mathbf{A}}_i^T \dot{\mathbf{A}}_i)$ (current paper)

Appendix K. RAD formulae in the literature

Giles [61] proposed the following RAD formula for singular value derivative

$$\bar{\mathbf{A}} = \mathbf{U}\bar{\mathbf{S}}\mathbf{V}^\top. \quad (\text{K.1})$$

This formula works with real-valued inputs and is only for the singular value derivative. For the singular vector, an approach was shown in [66] but no concrete implementable formula was proposed. Townsend [56] proposed the following RAD formula for singular variables derivative

$$\begin{aligned} \bar{\mathbf{A}} = & [\mathbf{U}(\mathbf{F} \circ [\mathbf{U}^\top \bar{\mathbf{U}} - \bar{\mathbf{U}}^\top \mathbf{U}])\mathbf{S} + (\mathbf{I}_m - \mathbf{U}\mathbf{U}^\top)\bar{\mathbf{U}}\mathbf{S}^{-1}]\mathbf{V}^\top \\ & + \mathbf{U}(\mathbf{I}_k \circ \bar{\mathbf{S}})\mathbf{V}^\top + \mathbf{U}[\mathbf{S}(\mathbf{F} \circ [\mathbf{V}^\top \bar{\mathbf{V}} - \bar{\mathbf{V}}^\top \mathbf{V}])\mathbf{V}^\top + \mathbf{S}^{-1}\bar{\mathbf{V}}^\top(\mathbf{I}_n - \mathbf{V}\mathbf{V}^\top)], \end{aligned} \quad (\text{K.2})$$

where \mathbf{A} is an $m \times n$ matrix of rank $k \leq \min(m, n)$, \mathbf{U} is $m \times k$, \mathbf{S} is $k \times k$, \mathbf{V} is $n \times k$, $\mathbf{U}^\top \mathbf{U} = \mathbf{V}^\top \mathbf{V} = \mathbf{I}_k$ (the identity matrix of dimension k), and \mathbf{F} is defined as

$$\mathbf{F}_{ij} = \begin{cases} \frac{1}{s_j^2 - s_i^2} & \text{if } i \neq j, \\ 0 & \text{if } i = j, \end{cases} \quad (\text{K.3})$$

where s is each entry of the singular values matrix \mathbf{S} . Also, \circ denotes the Haddamard product. This formula works with truncated SVD and also with only real-valued inputs and outputs. Wan and Zhang [58] proposed the following RAD formula

$$\begin{aligned} \bar{\mathbf{A}} = & \frac{1}{2} \left(2\mathbf{U}\bar{\mathbf{S}}\mathbf{V}^* + \mathbf{U}(\mathbf{J} + \mathbf{J}^*)\mathbf{S}\mathbf{V}^* + \mathbf{U}\mathbf{S}(\mathbf{K} + \mathbf{K}^*)\mathbf{V}^* + \frac{1}{2}\mathbf{U}\mathbf{S}^{-1}(\mathbf{L}^* - \mathbf{L})\mathbf{V}^* \right. \\ & \left. + 2(\mathbf{I} - \mathbf{U}\mathbf{U}^*)\bar{\mathbf{U}}\mathbf{S}^{-1}\mathbf{V}^* + 2\mathbf{U}\mathbf{S}^{-1}\bar{\mathbf{V}}^*(1 - \mathbf{V}\mathbf{V}^*) \right), \end{aligned} \quad (\text{K.4})$$

where $\mathbf{J} = \mathbf{F} \circ (2\mathbf{U}^*\bar{\mathbf{U}})$, $\mathbf{K} = \mathbf{F} \circ (2\mathbf{V}^*\bar{\mathbf{V}})$, $\mathbf{L} = \mathbf{I} \circ (2\mathbf{V}^*\bar{\mathbf{V}})$, \mathbf{F} is same as in Eq. (K.3), \mathbf{I} is the identity matrix. The formula proposed works with complex valued inputs and gives one single derivative value as opposed to the complex components shown in the current manuscript (such as $df_r/d\mathbf{A}_r$). The details on this Wirtinger derivative are shown in Appendix L.

Seeger et al [57] proposed the following RAD formula for singular variables

derivative

$$\begin{aligned}
\bar{\mathbf{A}} &= \mathbf{U}^\top (\mathbf{G}_2 \mathbf{V} + \Lambda^{-1} \bar{\mathbf{V}}), \\
\mathbf{G}_2 &= \mathbf{G}_1 \circ \mathbf{E} \Lambda - (\Lambda^{-1} \bar{\mathbf{V}} \mathbf{V}^\top \circ \mathbf{I}), \\
\mathbf{G}_1 &= \bar{\mathbf{U}} \mathbf{U}^\top + \Lambda^{-1} \bar{\mathbf{V}} \mathbf{V}^\top \mathbf{A}, \\
\mathbf{E}_{i,j} &= \begin{cases} \frac{1}{\lambda_j - \lambda_i}, & i \neq j, \\ 0, & i = j, \end{cases} \quad h(t) = \max(|t|, \epsilon) \operatorname{sgn}(t),
\end{aligned} \tag{K.5}$$

where the singular value decomposition (SVD) in Seeger et al [57] is defined as

$$\mathbf{A} = \mathbf{U}^\top \Lambda \mathbf{V}, \quad \Lambda = \operatorname{diag}(\lambda) \in \mathbb{R}^{m \times m}, \quad \mathbf{U} \in \mathbb{R}^{m \times m}, \quad \mathbf{V} \in \mathbb{R}^{m \times n}, \tag{K.6}$$

and further details on the computation of thin SVD can be found in Seeger et al [57]. The formula in Eq. (K.5) works with real valued inputs.

Appendix L. Wirtinger derivative

In the current manuscript just as in He et al. [42], the derivatives in the complex domain are expressed in terms of their real and imaginary components as $df_r/d\mathbf{A}_r$ and such. It may therefore be useful to the readers to see one single derivative $df/d\mathbf{A}$ for the complex valued case. This can be achieved by using the Wirtinger derivative. Information on this derivative can be found in the book by Hjørungnes [67]. The derivative is

$$\frac{df}{d\mathbf{A}} = \frac{1}{2} \left(\frac{df_r}{d\mathbf{A}_r} + i \frac{df_i}{d\mathbf{A}_r} - i \frac{df_r}{d\mathbf{A}_i} + \frac{df_i}{d\mathbf{A}_i} \right), \tag{L.1}$$

where i is iota, the complex number $\sqrt{-1}$.

For instance, take the singular value derivative as shown in Eqs. (F.7) and (F.9). These go into the Wirtinger derivative as shown below

$$\frac{d\sigma}{d\mathbf{A}} = \frac{1}{2} \left[\frac{\partial \sigma_r}{\partial \mathbf{A}_r} - i \frac{\partial \sigma_r}{\partial \mathbf{A}_i} \right]. \tag{L.2}$$

The imaginary terms for the singular value have been removed in Eq. (L.2) because the singular value is purely real. Before we proceed, consider the

following equation:

$$\mathbf{u}\mathbf{v}^* = (\mathbf{u}_r + i\mathbf{u}_i)(\mathbf{v}_r^\top - i\mathbf{v}_i^\top) = (\mathbf{u}_r\mathbf{v}_r^\top + \mathbf{u}_i\mathbf{v}_i^\top) + i(\mathbf{u}_i\mathbf{v}_r^\top - \mathbf{u}_r\mathbf{v}_i^\top). \quad (\text{L.3})$$

We will then use Eq. (F.7) and Eq. (F.9) to expand Eq. (L.2). After doing so, we obtain:

$$\frac{d\sigma}{d\mathbf{A}} = \frac{1}{2} \left[(\mathbf{u}_r\mathbf{v}_r^\top + \mathbf{u}_i\mathbf{v}_i^\top) - i(\mathbf{u}_i\mathbf{v}_r^\top - \mathbf{u}_r\mathbf{v}_i^\top) \right]. \quad (\text{L.4})$$

Upon careful observation, one can notice that the term square in brackets of Eq. (L.4) is simply the complex conjugate of Eq. (L.3). Thus, we have

$$\frac{d\sigma}{d\mathbf{A}} = \frac{1}{2}(\mathbf{u}\mathbf{v}^*)^c, \quad (\text{L.5})$$

where c denotes complex conjugate operation. In this way, we can compute the derivative of any one particular singular value with respect to its complex matrix \mathbf{A} . The formula however must not be confused with the formula in the real case. This is because the Wirtinger derivative is only applied in the complex plane treating the complex variable and its complex conjugate variable as two independent variables [68]. Similarly, we can compute the total derivative from the complex parts in Eqs. (20), (25) and (28).